

Gluon Sivers function in dijet production at the EIC

Miguel G. Echevarria,^{a,b} Patricia Andrea Gutierrez García,^c Ignazio Scimemi^c

^a*Department of Physics, University of the Basque Country UPV/EHU, 48080 Bilbao, Spain*

^b*EHU Quantum Center, University of the Basque Country UPV/EHU*

^c*Dpto. de Física Teórica & IPARCOS, Universidad Complutense de Madrid, Plaza de Ciencias 1, E-28040 Madrid, Spain*

E-mail: miguel.garciae@ehu.es, patricgu@ucm.es, ignazios@ucm.es

ABSTRACT: The transverse-momentum-dependent (TMD) factorization theorem for dijet production in deep-inelastic scattering is used here to make predictions of the gluon Sivers function. We revise the previously studied unpolarized case and develop the formalism for a transversely polarized target. We study the impact of TMD evolution in two different schemes and we use the current extractions of the evolution kernel at N³LO to make predictions for the future Electron-Ion Collider (EIC). The results strongly depend on the TMD gluon distributions and their evolution kernel. Big values of the Sivers asymmetry at the EIC are predicted, between 5-50%.

Contents

1	Introduction	2
2	Notation and kinematics	3
3	Factorization for the dijet cross section in SIDIS	5
3.1	Gluon channel	6
3.2	Quark/anti-quark channels	7
3.3	Weighted cross section and Sivers asymmetry	8
4	Operator definitions	9
5	Renormalization group equations and evolution kernels	11
6	Evolution kernel for the soft and collinear-soft function: \mathcal{M}-scheme	13
6.1	Scale fixing and non-perturbative effects	14
6.2	Final expression of the unpolarized hadronic tensor	17
6.3	Final expression of the hadronic tensor for Sivers function measurement	17
6.4	\mathcal{M} -function scheme at one loop	18
7	The quark and gluon CS-kernels for evolution	20
8	Sivers function models	21
8.1	Models for quark Sivers function	21
8.1.1	Model BPV	21
9	Results	22
10	Conclusions	24
A	Appendix	26
A.1	\mathcal{M} -function saddle point	26
A.2	Angular integrals	26
B	Hard prefactors	27
C	Anomalous dimensions	29
D	Sivers fit parameters	29
E	Model EKT	29

1 Introduction

The information about quark and gluon nonperturbative dynamics available in transverse momentum differential cross sections is currently expressed in terms of transverse momentum dependent distributions (TMDs) and collinear distributions (PDF or fragmentation functions) [1]. Both depend on collinear momentum fractions and only TMD distributions include a dependence on quark or gluon transverse momenta. The TMD distributions are obtained in the framework of TMD factorization (see [2–6] for a general treatment with different methods). In this work we will take the case of dijet production in semi-inclusive deep inelastic scattering (SIDIS). Dijets have been studied in the small- x limit in [7–10].

The TMD factorization of dijet production in SIDIS was shown in [11, 12] using Soft Collinear Effective Theory (SCET) [13–16] (see [17] for an introduction). The factorization theorem reported in those works is readily applicable to the case of polarized targets that allow the study of the gluon Sivers function. Several technical issues however deserve a special study that we treat in the present work.

Dijet production is highly sensitive to both quark and gluon TMDs and for this reason it is of most interest at future Electron-Ion Collider (EIC) [18]. At leading power in transverse momentum and leading order in perturbation theory, both quark and gluon channels contribute (while in single jet SIDIS the gluon effects appear just as corrections in both expansions [19–22]). We consider the cases of polarized and unpolarized targets. The former allows access to the T-odd gluon Sivers TMD ($f_{1T}^{\perp g}$). This function describes the distribution of unpolarized gluons in a transversely polarized nucleon and can be essential in other studies of transverse single-spin asymmetries (see e.g. [23]). A classification of all gluon TMDs can be found in [24]. The gluon momentum distributions inside a hadron are notoriously difficult to extract from experimental data. The difficulty comes mainly from the fact that they appear together with light quark distributions that often dominate the processes. Some early attempts to extract the gluon Sivers functions can be found in [25–27], which however do not provide a detailed discussion of factorization nor include TMD evolution effects. In general the processes which are more sensitive to gluon distributions include quarkonia production (as in measurements at the LHCspin facility [28]), open di-heavy quark, dijet and di-hadron production in semi-inclusive deep inelastic scattering (SIDIS) [29–35]. At present, there is no established model for the nonperturbative part of the gluon Sivers function, but there are studies dedicated to this issue e.g. [36].

The TMD evolution used in this work is defined by the so called ζ -prescription [37] and it is provided by the code `artemide` [38]. This has been successfully tested in fits of unpolarized distributions in Drell-Yan and SIDIS [39–43] and polarized quark Sivers distributions [44] including a perturbative TMD evolution kernel up to next-to-next-to-next-to leading order (N³LO). The availability of (quark and gluon) unpolarized and (quark) Sivers TMD functions extracted from data within a single scheme at high perturbative order results to be advantageous with respect to other extractions that do not offer a complete treatment of both unpolarized and Sivers cases in the same setup (see the extractions of unpolarized functions in ref. [45–47]).

In the present work we observe that we can define two possible schemes to implement TMD evolution. Out of these, one was already proposed in ref. [12] (we will call it "CCS-scheme") and one is proposed here for the first time (we will call it " \mathcal{M} -scheme"). The difference comes from implementing the ζ -prescription and renormalization set-up scales in two different ways. In the CCS-

scheme one defines a ζ -prescription condition for soft function appearing in the dijet factorization theorem independently from the renormalization scales of the collinear-soft functions. In the \mathcal{M} -scheme one defines an \mathcal{M} -function as the product of the collinear-soft and soft functions appearing in the dijet factorization theorem and the ζ -prescription and renormalization scales are defined for the \mathcal{M} -function. The \mathcal{M} -scheme is here tested for the first time on unpolarized and Sivers cross sections. The results of the two schemes are consistent within errors, but the \mathcal{M} is technically simpler and avoids several constraints on renormalization scale choices that were found in ref. [12].

As a technical aspect, we have currently two different values of the nonperturbative part of the evolution kernel in the `artemide` code. In fact we have two possible extractions, one which used only Drell-Yan data [42] and one which used Drell-Yan plus SIDIS data [43]. The TMD evolution kernel is universal, however for the moment there is some tension between the two extractions that has not been fully understood yet. We check the prediction for the Sivers asymmetry in the two cases.

Concerning the model for gluon Sivers functions we make some controlled assumptions and quantify uncertainties. As default we consider gluon Sivers functions equal to the sea-quark contributions obtained in fits of the Sivers asymmetry [44] that we comment later in the text. The associated uncertainty is still definitely large, but nevertheless the results that we get provide valuable information.

The work notation is defined in sec. 2. The expressions for the factorized cross section for SIDIS are in sec. 3. Here we give details on both quark and gluon channel contributions to the cross section. The definition of the operators that appear in the cross section is reported in sec. 4. The evolution differential equations and the formal expression of the cross sections including the evolution kernels are reported in sec. 5. In section 6 we provide the definition of the \mathcal{M} -scheme and the final expressions for the hadronic tensors in all schemes. Sections 7 and 8 review Collins-Soper kernel and Sivers function models extractions respectively. The results of this work are discussed in sec. 9 and we conclude in sec. 10. Some technical formulas are left for the appendix.

2 Notation and kinematics

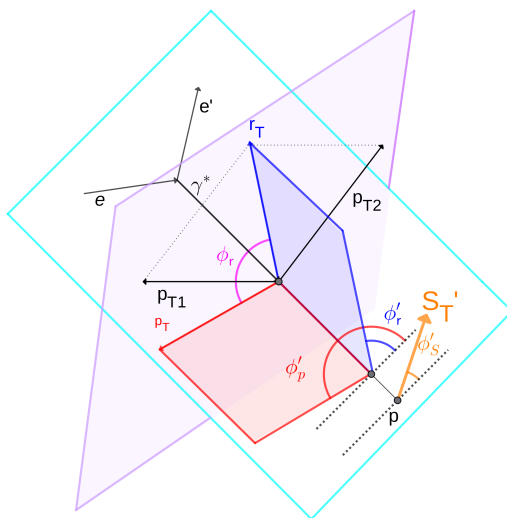


Figure 1: Planes and angles for dijet production in SIDIS in the Breit frame

In this work, we study dijet production in hadron-lepton collisions, with the initial hadron being transversely polarized:

$$\ell + h(P, \uparrow) \rightarrow \ell' + J_1(p_1) + J_2(p_2) + X. \quad (2.1)$$

We work in the Breit frame where both the virtual photon and the beam hadron scatter along the z-axis. A schematic view of the process is provided in fig. 1. We use light-cone coordinates to express four-vectors in terms of their “plus,” “minus,” and transverse components, specifically:

$$p^\mu = p_+ \bar{n}^\mu + p_- n^\mu + p_\perp^\mu = (p_+, p_-, \mathbf{p}_\perp), \quad (2.2)$$

with $n^\mu = (1, 0, 0, 1)/\sqrt{2}$, $\bar{n}^\mu = (1, 0, 0, -1)/\sqrt{2}$,

$$p_+ = n \cdot p, \quad p_- = \bar{n} \cdot p, \quad p^2 = 2p_+ p_- + p_\perp^\mu p_{\mu,\perp} = 2p_+ p_- - \mathbf{p}_\perp^2, \quad p_T = |\mathbf{p}_\perp|, \quad (2.3)$$

where the four-vector n^μ and \bar{n}^μ satisfy the relation $n \cdot \bar{n} = 1$ with $n^2 = \bar{n}^2 = 0$. The light-cone directions of the two jets are given by v_1 and v_2 . For each of these vector one can define a conjugate one ($\bar{v}_{1,2}$) such that

$$v_J^2 = \bar{v}_J^2 = 0, \quad v_J \cdot \bar{v}_J = 1, \quad \text{with } J = 1, 2, \quad (2.4)$$

The jets momenta $p_{1,2}^\mu$ have components transverse to the beam axis, $\mathbf{p}_{1\perp}$ and $\mathbf{p}_{2\perp}$. These momenta can be used to define the jet imbalance \mathbf{r}_\perp and the hard transverse momentum, \mathbf{p}_\perp ,

$$\mathbf{r}_\perp = \mathbf{p}_{1\perp} + \mathbf{p}_{2\perp}, \quad r_T = |\mathbf{r}_\perp|, \quad \text{and } \mathbf{p}_\perp = \frac{\mathbf{p}_{1\perp} - \mathbf{p}_{2\perp}}{2}, \quad p_T = |\mathbf{p}_\perp|. \quad (2.5)$$

At Born level $\mathbf{p}_{1\perp} = -\mathbf{p}_{2\perp}$ and thus $\mathbf{r}_\perp = 0$. In general the TMD factorization theorem is valid when $r_T \ll p_T$. Following a similar notation for the Fourier conjugate variable of \mathbf{r}_\perp called \mathbf{b}_\perp we can define $b^\mu = (0, \mathbf{b}_\perp, 0)$, $b_T = |\mathbf{b}_\perp|$. Similar plane projections are used in [48–50].

Other important variables are the Bjorken momentum fraction (x), the total invariant mass squared (s) and the inelasticity (y) defined as

$$x = \frac{Q^2}{2P \cdot q}, \quad s = (\ell + P)^2, \quad y = \frac{q \cdot P}{\ell \cdot P} = \frac{Q^2}{xs}, \quad (2.6)$$

with $Q^2 = -q^2 = -(\ell - \ell')^2$, q^μ the momentum of the virtual photon and P^μ the momentum of the target hadron. In the Breit frame and neglecting mass corrections we have that the momentum associated to the virtual photon and the target hadron are:

$$q^\mu = (0, 0, 0, Q), \quad P^\mu = \frac{1}{2x}(Q, 0, 0, -Q). \quad (2.7)$$

The ratio of the longitudinal momenta of the incoming parton and the target hadron is denoted by $\xi = k^+/P^+$ where k^μ is the momenta of the parton incoming to the hard process. Using the pseudorapidities, η_1 and η_2 , of the outgoing jets, we obtain the following relations for the partonic variables,

$$\begin{aligned} \hat{s} &= (q + k)^2 = +4p_T^2 \cosh^2(\eta_-), \\ \hat{t} &= (q - p_2)^2 = -4p_T^2 \cosh(\eta_-) \cosh(\eta_+) \exp(\eta_1), \\ \hat{u} &= (q - p_1)^2 = -4p_T^2 \cosh(\eta_-) \cosh(\eta_+) \exp(\eta_2), \\ Q^2 &= -(\hat{s} + \hat{t} + \hat{u}), = 2p_T^2 \cosh(\eta_-) \exp(\eta_+), \\ \xi &= 2x \cosh(\eta_+) \exp(-\eta_+) \quad \text{with } \eta_\pm = \frac{\eta_1 \pm \eta_2}{2}. \end{aligned} \quad (2.8)$$

The relations among angles in Breit frame shown in fig. 1 is

$$\phi_r = \phi'_r - \phi'_p, \quad \phi_S = \phi'_S - \phi'_p, \quad (2.9)$$

where ϕ'_S , ϕ'_r and ϕ'_p are measured w.r.t. the lepton plane and they are the azimuthal angles of transverse spin vector of the incoming proton \mathcal{S}_T , jet imbalance \mathbf{r}_\perp and average transverse momenta of the jets \mathbf{p}_\perp , respectively. As we will see later in the next section, in order to measure the Sivers function, one needs to look at the $\sin(\phi_S - \phi_r)$ modulated cross section. In the following, we summarize the factorization formalism for dijet production in SIDIS.

3 Factorization for the dijet cross section in SIDIS

The goal of this section is to obtain a factorized cross section for dijet production in SIDIS when the jet imbalance \mathbf{r}_\perp is small with respect to the hard scale transverse momentum of the jets, that is, when the factorization condition is $r_T \ll p_T$ and the virtual photon and target-hadron directions are back-to-back (Breit frame). For the EIC case this condition is fulfilled for $p_T \in [5, 40]$ GeV and in the central rapidity region as studied in [12]. We also assume that there is no hierarchy between the partonic Mandelstam variables, i.e. $\hat{s} \sim |\hat{t}| \sim |\hat{u}|$. Outside this region there are large logarithms in the hard factor of the cross-section which potentially would ruin the convergence of perturbative expansion. Under the proper factorization conditions, the dijet cross-section is given by

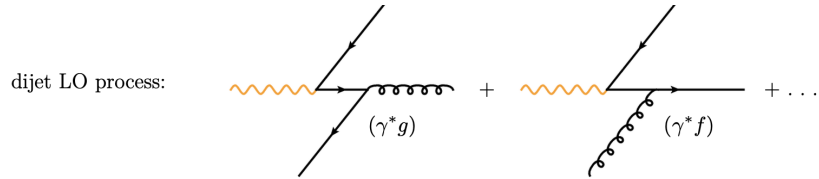


Figure 2: Dijet hard processes at leading order, from [11]. Here $f = q, \bar{q}$.

$$\frac{d\sigma}{d\Pi d\mathbf{r}_\perp} \equiv \frac{d\sigma}{dx d\eta_1 d\eta_2 dp_T d\mathbf{r}_\perp} = d\sigma(\phi_S, \phi_r) = d\sigma^U(\phi_r) + d\sigma^T(\phi_S, \phi_r), \quad (3.1)$$

where all variables are defined in sec. 2 and

$$d\Pi = dx d\eta_1 d\eta_2 dp_T. \quad (3.2)$$

In eq. (3.1), $d\sigma^U$ corresponds to the case of scattering from an unpolarized hadron, while $d\sigma^T$ arises when the hadron is transversely polarized. We do not treat here the case of longitudinally polarized hadrons, as discussed later in sec. 3.1. The formalism for factorization follows [11] for the unpolarized case, see also fig. 2. For each piece of the cross section we have two contributions coming from photon-gluon and photon-quark/anti-quark scattering

$$d\sigma^{U,T} = d\sigma^{U,T}(\gamma^*g) + \sum_{q=\text{flav.}} d\sigma^{U,T}(\gamma^*q) + \sum_{\bar{q}=\text{flav.}} d\sigma^{U,T}(\gamma^*\bar{q}) \quad (3.3)$$

and "flav." stands for quark flavors. In the following we describe (γ^*g) and (γ^*q) channels one by one.

3.1 Gluon channel

For the gluon channel the differential cross-section is expressed as :

$$\begin{aligned} \frac{d\sigma(\gamma^*g)}{d\Pi d\mathbf{r}_\perp} &= \sum_q H_{\gamma^*g \rightarrow q\bar{q}}^{\mu\nu}(\mu) \int \frac{d^2\mathbf{b}_\perp}{(2\pi)^2} \exp(i\mathbf{b}_\perp \cdot \mathbf{r}_\perp) F_{g,\mu\nu}(\xi, \mathbf{b}_\perp, \mu, \zeta_1) \\ &\times S_{\gamma g}(\mathbf{b}_\perp, \eta_1, \eta_2, \mu, \zeta_2) C_q(\mathbf{b}_\perp, R, \mu) J_q(p_T, R, \mu) C_{\bar{q}}(\mathbf{b}_\perp, R, \mu) J_{\bar{q}}(p_T, R, \mu). \end{aligned} \quad (3.4)$$

where $F_g^{\mu\nu}$ is the TMD gluon tensor, $H_{\gamma^*g \rightarrow q\bar{q}}^{\mu,\nu}$ is the gluon hard tensor, $S_{\gamma g}$ denotes the dijet soft function and $J_{q(\bar{q})}$ and $C_{q(\bar{q})}$ are the quark jet and collinear-soft functions. Notice that the TMD are evaluated at ξ given in sec. 2. The explicit definition of $S_{\gamma g}$, $J_{q(\bar{q})}$, $C_{q(\bar{q})}$ as matrix element of operators is reported in sec. 4. Finally, μ is the factorization scale, and ζ_i 's are the rapidity scales typical of TMD factorization. All scales cancel in the product of all these functions with the condition $\zeta_1\zeta_2 = p_T^2$, see [11]. The variable ξ is the Bjorken collinear momentum fraction and R is the jet radius (we assume to be the same for both jets).

The gluon hard tensor $H^{\mu\nu}(\mu)_{\gamma^*g \rightarrow q\bar{q}}$ incorporates contributions from both unpolarized ($\propto H_{\gamma^*g \rightarrow q\bar{q}}^{Ug}$) and linearly polarized gluons ($\propto H_{\gamma^*g \rightarrow q\bar{q}}^{Lg}$) and it does not depend on hadron polarization:

$$H_{\gamma^*g \rightarrow q\bar{q}}^{\mu\nu} = \sigma_0^{gU} H_{\gamma^*g \rightarrow q\bar{q}}^{Ug} \frac{g_\perp^{\mu\nu}}{d-2} + \sigma_0^{gL} H_{\gamma^*g \rightarrow q\bar{q}}^{Lg} \left(-\frac{g_\perp^{\mu\nu}}{d-2} + \frac{v_{1\perp}^\mu v_{2\perp}^\nu + v_{2\perp}^\mu v_{1\perp}^\nu}{2 v_{1\perp} \cdot v_{2\perp}} \right). \quad (3.5)$$

The hard prefactors are reported in appendix B. Linearly polarized gluons result to be α_s^2 suppressed in the matching with collinear distributions [51] so that we neglect them and we use

$$H_{\gamma^*g \rightarrow q\bar{q}}^{\mu\nu} \simeq \sigma_0^{gU} H_{\gamma^*g \rightarrow q\bar{q}}^{Ug} \frac{g_\perp^{\mu\nu}}{d-2} \quad (3.6)$$

The transverse momentum-dependent (TMD) gluon tensor $F_g^{\mu\nu}$ can be also decomposed into unpolarized and linearly polarized parts,

$$\begin{aligned} F_{g/A}^{\mu\nu[U]}(\xi, \mathbf{r}_\perp) &= g_\perp^{\mu\nu} f_1^g(\xi, r_T) + \dots, \\ F_{g/A}^{\mu\nu[T]}(\xi, \mathbf{r}_\perp) &= -g_\perp^{\mu\nu} \frac{\epsilon_\perp^{\alpha\beta} r_{\perp\alpha} S_{\perp\beta}}{M} f_{1T}^{\perp g}(\xi, r_T) + \dots \end{aligned} \quad (3.7)$$

and the dots include TMDs that do not enter this work. see for instance ref. [52, 53]¹. We use $\epsilon_{0123} = -\epsilon^{0123} = 1$, and $\epsilon_\perp^{12} = -\epsilon_\perp^{21} = 1$ so that $\epsilon_\perp^{\alpha\beta} r_{\perp\alpha} S_{\perp\beta} = r_T S_T \sin(\phi_S - \phi_r)$. Using the Fourier transform definition,

$$G_{g/A}^{\mu\nu[pol]}(\xi, \mathbf{b}_\perp) = \int d^2\mathbf{r}_\perp e^{-i\mathbf{r}_\perp \cdot \mathbf{b}_\perp} G_{g/A}^{\mu\nu[pol]}(\xi, \mathbf{r}_\perp), \quad (3.8)$$

we have

$$\begin{aligned} F_{g/A}^{\mu\nu[U]}(\xi, \mathbf{b}_\perp) &= g_\perp^{\mu\nu} f_1^g(\xi, b_T) + \dots, \\ F_{g/A}^{\mu\nu[T]}(\xi, \mathbf{b}_\perp) &= +i g_\perp^{\mu\nu} \epsilon_\perp^{\alpha\beta} M b_{\perp\alpha} S_{\perp\beta} f_{1T}^{\perp g}(\xi, b_T) + \dots \end{aligned} \quad (3.9)$$

¹In the definition of [53] the gluon distributions are multiplied by a factor $\xi(x)$, because of a different normalization of the matrix element definition. We use the operator definition of sec. 4.

and $\epsilon_{\perp}^{\alpha\beta} b_{\perp\alpha} S_{\perp\beta} = b_T S_T \sin(\phi_S - \phi_b)$. The Fourier transforms are

$$\begin{aligned} f_1^g(\xi, b_T) &= 2\pi \int_0^{\infty} dr_T r_T J_0(b_T r_T) f_1^g(\xi, r_T), \\ f_{1T}^{\perp g}(\xi, b_T) &= \frac{2\pi}{M^2} \int_0^{\infty} dr_T \frac{r_T^2}{b_T} J_1(b_T r_T) f_{1T}^{\perp g}(\xi, r_T) \end{aligned} \quad (3.10)$$

where J_n is the Bessel function of the first kind of order n and it is defined as

$$J_n(z) = \frac{1}{2\pi i^n} \int_0^{2\pi} d\varphi \exp(in\varphi + iz\cos\varphi).$$

Separating the cross section for unpolarized and polarized hadron targets the cross section for the gluon channel is,

$$\frac{d\sigma(\gamma^*g)}{d\Pi d\mathbf{r}_{\perp}} = \frac{d\sigma^U(\gamma^*g)}{d\Pi d\mathbf{r}_{\perp}} + \frac{d\sigma^T(\gamma^*g)}{d\Pi d\mathbf{r}_{\perp}}. \quad (3.11)$$

Using

$$F_{g,\mu\nu}^U H_{\gamma^*g \rightarrow q\bar{q}}^{\mu\nu} = \sigma_0^{gU} H_{\gamma^*g \rightarrow q\bar{q}}^U f_1^g(\xi, b), \quad (3.12)$$

the unpolarized part agrees with [31, 54–56] and it is

$$\begin{aligned} \frac{d\sigma^U(\gamma^*g)}{d\Pi d\mathbf{r}_{\perp}} &= \sum_q \sigma_0^{gU} H_{\gamma^*g \rightarrow q\bar{q}}(\mu) \int \frac{d^2\mathbf{b}_{\perp}}{(2\pi)^2} \exp(i\mathbf{b}_{\perp} \cdot \mathbf{r}_{\perp}) f_1^g(\xi, b_T; \mu, \zeta_1) \\ &\times S_{\gamma g}(\mathbf{b}_{\perp}, \eta_1, \eta_2; \mu, \zeta_2) \mathcal{C}_q(\mathbf{b}_{\perp}, R; \mu) J_q(p_T, R, \mu) \mathcal{C}_{\bar{q}}(\mathbf{b}_{\perp}, R; \mu) J_{\bar{q}}(p_T, R; \mu), \end{aligned} \quad (3.13)$$

where ξ is related to x in eq. (2.8) and we have indicated explicitly the renormalization and rapidity scales (μ, ζ) . For the transversely polarized targets we have

$$F_{g,\mu\nu}^T H_{\gamma^*g \rightarrow f\bar{f}}^{\mu\nu} = +i S_T \sigma_0^{gU} H_{\gamma^*g \rightarrow f\bar{f}} \sin(\phi_S - \phi_b) f_{1T}^{\perp g}(\xi, b). \quad (3.14)$$

and the corresponding cross-section part:

$$\begin{aligned} \frac{d\sigma^T(\gamma^*g)}{d\Pi d\mathbf{r}_{\perp}} &= \sum_q (+i) \sigma_0^{gU} H_{\gamma^*g \rightarrow q\bar{q}}(\mu) \int \frac{d^2\mathbf{b}_{\perp}}{(2\pi)^2} \exp(i\mathbf{b}_{\perp} \cdot \mathbf{r}_{\perp}) S_T \sin(\phi_S - \phi_b) (b_T M) f_{1T}^{\perp g}(\xi, b_T; \mu, \zeta_1) \\ &\times S_{\gamma g}(\mathbf{b}_{\perp}, \eta_1, \eta_2; \mu, \zeta_2) \mathcal{C}_f(\mathbf{b}_{\perp}, R; \mu) J_f(p_T, R; \mu) \mathcal{C}_{\bar{f}}(\mathbf{b}_{\perp}, R; \mu) J_{\bar{f}}(p_T, R; \mu). \end{aligned} \quad (3.15)$$

3.2 Quark/anti-quark channels

The differential cross-section for the quark and anti-quark channels can be obtained one from the other just with the interchange of labels $q \leftrightarrow \bar{q}$. Thus, unless the notation creates confusion, in the following we limit ourselves to describe the quark case.

The quark cross section is

$$\begin{aligned} \frac{d\sigma(\gamma^*q)}{d\Pi d\mathbf{r}_{\perp}} &= \sigma_0^{fU} \sum_{q=\text{flav.}} H_{\gamma^*q \rightarrow gq}^U(\hat{s}, \hat{t}, \hat{u}; \mu) \int \frac{d^2\mathbf{b}_{\perp}}{(2\pi)^2} \exp(i\mathbf{b}_{\perp} \cdot \mathbf{r}_{\perp}) F_q(\xi, \mathbf{b}_{\perp}; \mu, \zeta_1) \\ &\times S_{\gamma q}(\mathbf{b}_{\perp}, \zeta_2; \mu) \mathcal{C}_g(\mathbf{b}_{\perp}, R; \mu) J_g(p_T, R; \mu) \mathcal{C}_q(\mathbf{b}_{\perp}, R; \mu) J_q(p_T, R; \mu), \end{aligned} \quad (3.16)$$

where the hard factor $H_{\gamma^*q \rightarrow gq}^U$ has the same functional form as in the unpolarized hadron case, and consistent with the absence of polarization in the final-state partons. The hard factor and the dijet soft function are the same for quarks and anti-quarks, i.e. $S_{\gamma q} = S_{\gamma \bar{q}}$. The quark TMD parton distribution function $F_q(\xi, b)$ is evaluated in ξ as in the the gluon channel case and it admits a decomposition into its unpolarized and Sivers-function components [57],

$$\begin{aligned} F_q(\xi, \mathbf{r}_\perp) &= F_q^{[U]}(\xi, \mathbf{r}_\perp) + F_q^{[T]}(\xi, \mathbf{r}_\perp), \\ F_q^{[U]}(\xi, \mathbf{r}_\perp) &= f_1(\xi, r_T) + \dots \\ F_q^{[T]}(\xi, \mathbf{r}_\perp) &= -\frac{\epsilon_\perp^{\alpha\beta} r_{\perp\alpha} S_{\perp\beta}}{M} f_{1T}^\perp(\xi, r_T) + \dots, \end{aligned} \quad (3.17)$$

where we have omitted the functions that are not considered in this work. The function f_1 represents the distribution of an unpolarized quark in an unpolarized hadron, and f_{1T}^\perp , the quark Sivers function, represents the distribution for an unpolarized quark in an polarized hadron. In conjugate space we have

$$\begin{aligned} F_q^{[U]}(\xi, \mathbf{b}_\perp) &= f_1(\xi, b_T) + \dots, \\ F_q^{[T]}(\xi, \mathbf{b}_\perp) &= +i\epsilon_\perp^{\alpha\beta} b_{\perp\alpha} S_{\perp\beta} M f_{1T}^\perp(\xi, b_T) + \dots. \end{aligned} \quad (3.18)$$

The Fourier transforms to pass from momentum to conjugate spaces are analogue to eq. 3.10. Using the decomposition in eq. (3.1) one gets

$$\frac{d\sigma^U(\gamma^*q)}{d\Pi d\mathbf{r}_\perp} = \sigma_0^{fU} \sum_{q=\text{flav.}} H_{\gamma^*q \rightarrow gq}^U(\hat{s}, \hat{t}, \hat{u}; \mu) \int \frac{d^2\mathbf{b}_\perp}{(2\pi)^2} \exp(i\mathbf{b}_\perp \cdot \mathbf{r}_\perp) f_1(\xi, b_T; \mu, \zeta_1) \quad (3.19)$$

$$\times S_{\gamma q}(\mathbf{b}_\perp, \zeta_2, \mu) \mathcal{C}_g(\mathbf{b}_\perp, R; \mu) J_g(p_T, R; \mu) \mathcal{C}_q(\mathbf{b}_\perp, R; \mu) J_q(p_T, R; \mu),$$

$$\frac{d\sigma^T(\gamma^*q)}{d\Pi d\mathbf{r}_\perp} = +i\sigma_0^{fU} \sum_{q=\text{flav.}} H_{\gamma^*q \rightarrow gq}^U(\hat{s}, \hat{t}, \hat{u}, \mu) \int \frac{d^2\mathbf{b}_\perp}{(2\pi)^2} \exp(i\mathbf{b}_\perp \cdot \mathbf{r}_\perp) S_T \sin(\phi_S - \phi_b)(b_T M)$$

$$\times f_{1T}^\perp(\xi, b_T; \mu, \zeta_1) S_{\gamma q}(\mathbf{b}_\perp, \zeta_2, \mu) \mathcal{C}_g(\mathbf{b}_\perp, R; \mu) J_g(p_T, R; \mu) \mathcal{C}_q(\mathbf{b}_\perp, R; \mu) J_q(p_T, R; \mu). \quad (3.20)$$

The symbols used for each functions are the same as in the gluon channel case.

3.3 Weighted cross section and Sivers asymmetry

It is useful to introduce a notation for angular integrated cross sections for the unpolarized and polarized cases, namely,

$$\begin{aligned} W^{UU} &= r_T \int_{-\pi}^{\pi} d\phi_r \frac{d\sigma^U}{d\Pi d\mathbf{r}_\perp} = \frac{d\sigma^U}{d\Pi dr_T}, \\ W^{UT} &= r_T \int_{-\pi}^{\pi} d\phi_r \sin(\phi_S - \phi_r) \frac{d\sigma^T}{d\Pi d\mathbf{r}_\perp}. \end{aligned} \quad (3.21)$$

We decompose $W^{UU,UT}$ according to quark and gluon initiated contributions,

$$W^{UU,UT} = W_g^{UU,UT} + \sum_{q=\text{flav.}} \left(W_q^{UU,UT} + W_{\bar{q}}^{UU,UT} \right). \quad (3.22)$$

For each channel the factorization formulas are schematically and respectively given by:

$$\begin{aligned}
W_g^{UU} &= r_T \int_{-\pi}^{\pi} d\phi_r \frac{d\sigma^T(\gamma^*g)}{d\Pi d\mathbf{r}_{\perp}} \\
&= r_T \sigma_0^{gU} \sum_{q=\text{flav.}} H_{\gamma^*g \rightarrow q\bar{q}}^U(\mu) \int \frac{b_T db_T}{2\pi} J_0(r_T b_T) \int_{-\pi}^{\pi} d\phi_b f_1^g(\xi, b) S_{\gamma g} \mathcal{C}_q \mathcal{C}_{\bar{q}} J_q J_{\bar{q}}, \\
W_q^{UU} &= r_T \int_{-\pi}^{\pi} d\phi_r \frac{d\sigma^T(\gamma^*q)}{d\Pi d\mathbf{r}_{\perp}} = r_T \sigma_0^{fU} H_{\gamma^*q \rightarrow gq}^U(\mu) \int \frac{b_T db_T}{(2\pi)} J_0(r_T b_T) \int_{-\pi}^{\pi} d\phi_b f_1(\xi, b_T) S_{\gamma q} \mathcal{C}_g \mathcal{C}_q J_g J_q,
\end{aligned} \tag{3.23}$$

and

$$\begin{aligned}
W_g^{UT} &= r_T \int_{-\pi}^{\pi} d\phi_r \sin(\phi_S - \phi_r) \frac{d\sigma^T(\gamma^*g)}{d\Pi d\mathbf{r}_{\perp}} = -r_T \sigma_0^{gU} \sum_{q=\text{flav.}} H_{\gamma^*g \rightarrow q\bar{q}}^U(\mu) \\
&\quad \times \int \frac{b_T db_T}{2\pi} J_1(r_T b) \int_{-\pi}^{\pi} d\phi_b \sin^2(\phi_S - \phi_b) S_T(b_T M) f_{1T}^{\perp g}(\xi, b_T) S_{\gamma g} \mathcal{C}_q \mathcal{C}_{\bar{q}} J_q J_{\bar{q}}, \\
W_q^{UT} &= r_T \int_{-\pi}^{\pi} d\phi_r \sin(\phi_S - \phi_r) \frac{d\sigma^T(\gamma^*q)}{d\Pi d\mathbf{r}_{\perp}} = -r_T \sigma_0^{fU} H_{\gamma^*q \rightarrow gq}^U(\hat{s}, \hat{t}, \hat{u}, \mu) \\
&\quad \times \int \frac{b_T db_T}{(2\pi)} J_1(r_T b_T) \int_{-\pi}^{\pi} d\phi_b \sin^2(\phi_S - \phi_b) S_T(b_T M) f_{1T}^{\perp}(\xi, b_T) S_{\gamma q} \mathcal{C}_g \mathcal{C}_q J_g J_q,
\end{aligned} \tag{3.24}$$

where we have not reported the argument of all functions for brevity. In the next section we provide a detailed definition of each matrix element entering these formulas. In the plots that we show as our results in sec. 9 we will show the partially integrated cross-sections,

$$\begin{aligned}
\frac{d\sigma^{UU}}{dr_T} &= \int d\eta_1 d\eta_2 \delta(\eta_1) \delta(\eta_2) \int dp_T \delta(p_T - p_T^0) \int_{x_{\min}}^{x_{\max}} dx W^{UU}, \\
\langle \frac{d\sigma^{UT}}{dr_T} \rangle &\equiv \int d\eta_1 d\eta_2 \delta(\eta_1) \delta(\eta_2) \int d\phi_r r_T \sin(\phi_S - \phi_r) \int dp_T \delta(p_T - p_T^0) \frac{d\sigma^{UT}}{d\mathbf{r}_T dp_T} \\
&= \int d\eta_1 d\eta_2 \delta(\eta_1) \delta(\eta_2) \int dp_T \delta(p_T - p_T^0) \int_{x_{\min}}^{x_{\max}} dx W^{UT},
\end{aligned} \tag{3.25}$$

and the values of the inputs are specified in sec. 9. The Siverson asymmetries in sec. 9 are then defined as the ratio

$$A_{[x_{\min}, x_{\max}]}^{\text{Sivers}} = \frac{\langle d\sigma^{UT} \rangle / dr_T}{d\sigma^{UU} / dr_T}. \tag{3.26}$$

4 Operator definitions

Each of the functions of the previous section is understood as free of rapidity divergences. This ensures that we are expressing it in terms of universal functions. This is achieved in the following

way. The TMD are defined starting from the operator definitions

$$\begin{aligned}
\hat{B}_q(x, \mathbf{b}_\perp) &= \frac{1}{2} \sum_X \int \frac{d\xi^+}{2\pi} e^{-ixp^-\xi^+} \left\{ T \left[\bar{q}_i \tilde{W}_n^T \right]_a \left(\frac{\xi}{2} \right) |X\rangle \gamma_{ij}^- \langle X| \bar{T} \left[\tilde{W}_n^{T\dagger} q_j \right]_a \left(-\frac{\xi}{2} \right) \right\}, \\
\hat{B}_{\bar{q}}(x, \mathbf{b}_\perp) &= \frac{1}{2} \sum_X \int \frac{d\xi^+}{2\pi} e^{-ixp^-\xi^+} \left\{ T \left[\tilde{W}_n^{T\dagger} q_j \right]_a \left(\frac{\xi}{2} \right) |X\rangle \gamma_{ij}^- \langle X| \bar{T} \left[\bar{q}_i \tilde{W}_n^T \right]_a \left(-\frac{\xi}{2} \right) \right\}, \\
\hat{B}_{g,\mu\nu}(x, \mathbf{b}_\perp) &= \frac{1}{xp^-} \sum_X \int \frac{d\xi^+}{2\pi} e^{-ixp^-\xi^+} \left\{ T \left[F_{-\mu} \tilde{W}_n^T \right]_a \left(\frac{\xi}{2} \right) |X\rangle \langle X| \bar{T} \left[\tilde{W}_n^{T\dagger} F_{-\nu} \right]_a \left(-\frac{\xi}{2} \right) \right\}, \quad (4.1)
\end{aligned}$$

where $\xi = (\xi^+, 0^-, \mathbf{b}_\perp)$. The repeated color indices a ($a = 1, \dots, N_c$ for quarks and $a = 1, \dots, N_c^2 - 1$ for gluons) are summed up and we have not introduced any renormalization scale in the arguments for simplicity. The functions written above are un-subtracted bare functions, that is, they still have an overlap with soft or opposite modes and are not renormalized. Using a δ -regulator [58–61] the zero-bin subtracted functions are obtained

$$\hat{B}_i^{\text{subt}}(x, \mathbf{b}_\perp, \mu, p^-\delta_+) = \frac{\hat{B}_i(x, \mathbf{b}_\perp, \mu, p^-/\delta^-)}{S_i(\mathbf{b}_\perp, \mu, \sqrt{\delta^+\delta^-})}, \quad \text{with } i = q, g \quad (4.2)$$

where S_i (S_i depends just on the quark and gluon $SU(3)_c$ representation, that is $S_q = S_{\bar{q}}$) is the back-to-back two-direction soft function for SIDIS and Drell-Yan processes [60, 61],

$$S_i(\mathbf{b}_\perp) = \frac{\text{Tr}}{N_c} \langle 0| T \left[S_{ni}^{T\dagger} \tilde{S}_{ni}^T \right] (0^+, 0^-, \mathbf{b}_\perp) \bar{T} \left[\tilde{S}_{ni}^{T\dagger} S_{ni}^T \right] (0)|0\rangle, \quad \text{with } i = q, g \quad (4.3)$$

and S_n^T and \tilde{S}_n^T are soft Wilson lines as defined in [61] for fundamental and adjoint color representations.

The TMD factorization [59, 60] is realized using the soft function property

$$S_i(\mathbf{b}_\perp, \mu, \sqrt{\delta^+\delta^-}) = (S_i(\mathbf{b}_\perp, \mu, \delta^+\nu))^{\frac{1}{2}} (S_i(\mathbf{b}_\perp, \mu, \delta^-/\nu))^{\frac{1}{2}}, \quad \text{with } i = q, g \quad (4.4)$$

where ν is an arbitrary positive scale that parametrizes the ambiguity in this splitting and that will be removed from the final result, introducing this way a constraint on the product of rapidity scales. The TMD is finally defined as

$$F_i^{\text{bare}}(\xi, \mathbf{b}_\perp, \mu, \zeta_1) = B_i^{\text{subt}}(\xi, \mathbf{b}_\perp, \mu, p^-\delta^+) S_i^{\frac{1}{2}}(\mathbf{b}_\perp, \mu, \delta^+\nu) \Bigg|_{\sqrt{2}p^-\nu \rightarrow \sqrt{\zeta_1}}, \quad \text{with } i = q, \bar{q}, g \quad (4.5)$$

Similar manipulations can be performed for the other soft functions of the process,

$$\begin{aligned}
\hat{S}_{\gamma g}(\mathbf{b}_\perp) &= \frac{1}{C_{FC_A}} \langle 0| S_{gn}^\dagger(\mathbf{b}_\perp, -\infty)_{ca'} \text{Tr} \left[S_{qv_2}(+\infty, \mathbf{b}_\perp) T^{a'} S_{qv_1}^\dagger(+\infty, \mathbf{b}_\perp) \right. \\
&\quad \left. \times S_{qv_1}(+\infty, 0) T^a S_{qv_2}^\dagger(+\infty, 0) \right] S_{gn}(0, -\infty)_{ac} |0\rangle, \quad (4.6)
\end{aligned}$$

and soft function corresponding to the case of incoming quark or antiquark that is obtained exchanging

$$\hat{S}_{\gamma q} = \hat{S}_{\gamma g}(n \leftrightarrow v_2). \quad (4.7)$$

In this case we have

$$S_{\gamma_i}^{\text{bare}}(\mathbf{b}_\perp, \mu, \zeta_2) = \frac{\hat{S}_{\gamma_i}(\mathbf{b}_\perp, \mu, \sqrt{A_n} \delta^+)}{S(\mathbf{b}_\perp, \mu, \sqrt{\delta^+ \delta^-})} S^{\frac{1}{2}}(\mathbf{b}_\perp, \mu, \delta^- / \nu) \Bigg|_{\nu/\sqrt{2A_n} \rightarrow \sqrt{\zeta_2}}, \quad \text{with } i = q, g \quad (4.8)$$

with $A_n = v_1 \cdot v_2 / [(n \cdot v_1)(n \cdot v_2)]$ and the l.h.s free of rapidity divergences. In practice \hat{B} and \hat{S}_{γ_i} can be re-written as a product of TMDs which are free of rapidity divergences, and we have the factorization condition

$$\zeta_1 \zeta_2 = \frac{(k^-)^2}{A_n} = \frac{\hat{u} \hat{t}}{\hat{s}} = p_T^2, \quad (4.9)$$

where \hat{s} , \hat{t} , and \hat{u} are the partonic Mandelstam variables, eq. (2.8). The combination $\zeta_1 \zeta_2$ is Lorentz invariant. Notice that in the present case ζ_2 is a dimensionless quantity but ζ_1 , as usual, has dimensions of mass squared. The natural way to choose the values of ζ_1 and ζ_2 is

$$\zeta_1 = p_T^2, \quad \zeta_2 = 1. \quad (4.10)$$

The other functions that appear in the cross section are defined as in [62]

$$\begin{aligned} \mathcal{C}_q(\mathbf{b}_\perp, R, \mu) &= \int d\mathbf{b}_\perp \exp(\mathbf{b}_\perp \cdot \mathbf{v} \bar{v} \cdot \partial) \frac{1}{N_R} \text{Tr} \langle 0 | T [U_n^\dagger W_t(0)] \Theta_{\text{alg}} \bar{T} [W_t^\dagger U_n(0)] | 0 \rangle, \\ J_{q,v}(v \cdot p, R, \mu) &= \frac{1}{2\sqrt{2}N_c} \text{Tr} \int d^4x e^{ipx} \langle 0 | \bar{\chi}_v(p) \not{p} \delta_{\text{alg}}(R) \chi_v(0) | 0 \rangle, \\ \eta_\perp^{\rho\nu} J_{g,v}(v \cdot p, R, \mu) &= -\frac{1}{(N_c^2 - 1)} \sum_{A=1}^{N_c^2 - 1} \int d^4x (\sqrt{2}\bar{v} \cdot p) e^{ipx} \langle 0 | B_v^{\eta_\perp \rho A}(x) \delta_{\text{alg}}(R) g B_v^{\eta_\perp \nu A}(0) | 0 \rangle, \end{aligned} \quad (4.11)$$

where the prefix η_\perp here refers to the plane orthogonal to v whose transverse components are obtained with the tensor $\eta_\perp^{\rho\nu} = g^{\rho\nu} - (v^\rho \bar{v}^\nu + \bar{v}^\nu v^\rho)$. These functions do not suffer from rapidity divergences and have a standard behavior under renormalization.

5 Renormalization group equations and evolution kernels

In this section we sum up the main properties of the anomalous dimensions that appear in the factorization theorem. The anomalous dimension of the dijet soft functions depend on the variable $c_b = \cos\phi_b = \mathbf{b}_\perp \cdot \mathbf{v}_{1\perp} / (b_T v_{1T})$. From previous equations and taking into account the rapidity scale dependence one finds that soft functions obey

$$\begin{aligned} \frac{d}{d\ln\mu} S_{\gamma_i}(b, \mu, \zeta_2) &= \gamma_{S_{\gamma_i}}(\mu, c_b) S_{\gamma_i}(b, \mu, \zeta_2), \\ \frac{d}{d\ln\zeta_2} S_{\gamma_i}(b, \mu, \zeta_2) &= -\mathcal{D}_i(b, \mu) S_{\gamma_i}(b, \mu, \zeta_2), \quad \text{with } i = q, g \end{aligned} \quad (5.1)$$

where \mathcal{D} is the Collins-Soper kernel and $(\gamma_{S_{\gamma_{\bar{q}}}}, \mathcal{D}_{\bar{q}}) = (\gamma_{S_{\gamma_q}}, \mathcal{D}_q)$. Similar equations hold for the TMD

$$\begin{aligned} \frac{d}{d\ln\mu} F_i(b, \mu, \zeta_1) &= \gamma_{F_i}(\mu) F_i(b, \mu, \zeta_1), \\ \frac{d}{d\ln\zeta_1} F_i(b, \mu, \zeta_1) &= -\mathcal{D}_i(b, \mu) F_i(b, \mu, \zeta_1), \quad \text{with } i = q, \bar{q}, g, \end{aligned} \quad (5.2)$$

with $\gamma_{F_q} = \gamma_{F_{\bar{q}}}$. Although apparently similar, eq. (5.2) is independent of the cosine $c_{\mathbf{b}}$ contrary to the dijet soft function case, eq. (5.1). The integration of the angle ϕ_b is non trivial and in principle can give rise to spurious complex terms in the resummation. Concerning the other function that appear in the factorization theorem we have

$$\begin{aligned}\frac{d}{d\ln\mu}H_{\gamma i} &= \gamma_{H_{\gamma i}}(\mu)H_{\gamma i}, \\ \frac{d}{d\ln\mu}\mathcal{C}_i &= \gamma_{\mathcal{C}_i}(\mu, c_{\mathbf{b}}, R)\mathcal{C}_i, \\ \frac{d}{d\ln\mu}J_{\gamma i} &= \gamma_{J_i}(\mu, R)J_i \quad \text{with } i = q, \bar{q}, g,\end{aligned}\tag{5.3}$$

where we have made explicit also the dependence on the jet radius R and $c_{\mathbf{b}}$. Consistency of the cross section requires (here γ_α is from the a_s in the hard factor [11]),

$$\begin{aligned}\gamma_{H_{\gamma g}}(\mu) + \gamma_\alpha(\mu) + \gamma_{F_g}(\mu) + \gamma_{J_q}(\mu, R) + \gamma_{J_{\bar{q}}}(\mu, R) + \gamma_{\mathcal{C}_q}(\mu, c_{\mathbf{b}}, R) + \gamma_{\mathcal{C}_{\bar{q}}}(\mu, c_{\mathbf{b}}, R) + \gamma_{S_{\gamma g}}(\mu, c_{\mathbf{b}}) &= 0, \\ \gamma_{H_{\gamma q}}(\mu) + \gamma_\alpha(\mu) + \gamma_{F_q}(\mu) + \gamma_{J_q}(\mu, R) + \gamma_{J_g}(\mu, R) + \gamma_{\mathcal{C}_q}(\mu, c_{\mathbf{b}}, R) + \gamma_{\mathcal{C}_g}(\mu, c_{\mathbf{b}}, R) + \gamma_{S_{\gamma q}}(\mu, c_{\mathbf{b}}) &= 0.\end{aligned}\tag{5.4}$$

The one loop values of these anomalous dimensions can be found in the appendix C. Looking at this equations one can see that if the dijet soft and collinear-soft functions are evolved from the same initial to the same final scale the $c_{\mathbf{b}}$ dependence in the anomalous dimensions cancels altogether making the evolution simpler and well defined. Nevertheless one should still check the convergence of the perturbative series when such a choice is made. We discuss more this point in the next sections.

The evolution kernels that are obtained solving the renormalization group equations of each functions can be grouped together using factors $\mathcal{R}_{q,g}$ in the $W^{UU,UT}$ obtained in sec. 3.

For the unpolarized cross sections we have

$$\begin{aligned}W_g^{UU} &= r_T \sum_{q=\text{flav.}} \sigma_0^g H_{\gamma^* g \rightarrow q\bar{q}}(\mu)|_{\mu=p_T} (J_q(p_T, R, \mu_J) J_{\bar{q}}(p_T, R, \mu_J)) | \\ &\times \int_0^{+\infty} bdb J_0(br_T) f_1^g(\xi, \mathbf{b}) \mathcal{R}_g \left((\{\mu_k\}, \zeta_{1,0}, \zeta_{2,0}) \rightarrow (p_T, p_T^2, 1) \right) \hat{\sigma}_g^U(b, R, \{\mu_i\}),\end{aligned}\tag{5.5}$$

$$\begin{aligned}W_q^{UU} &= r_T \sigma_0^f H_{\gamma^* f \rightarrow g f}(\mu)|_{\mu=p_T} (J_q(p_T, R, \mu_J) J_g(p_T, R, \mu_J)) \\ &\times \int_0^{+\infty} bdb J_0(br_T) f_1^f(\xi, \mathbf{b}) \mathcal{R}_q \left((\{\mu_k\}, \zeta_{1,0}, \zeta_{2,0}) \rightarrow (p_T, p_T^2, 1) \right) \hat{\sigma}_q^U(b, R, \{\mu_i\}),\end{aligned}\tag{5.6}$$

and $\hat{\sigma}_{f,g}^U$ indicate the ϕ_b -integrated product of collinear-soft and soft functions, see eq. (3.23). Similar equations can be written for the polarized case with trivial changes in the labels and ϕ_b integrations for TMD distributions and the other functions, see eq. (3.24). The evolution kernels $\mathcal{R}_{q,g}$ in eq. (5.5-5.6) are the same in the polarized and unpolarized cases. They can be written as

$$\begin{aligned}\mathcal{R}_g \left((\{\mu_k\}, \zeta_{1,0}^g, \zeta_{2,0}^{S_{\gamma q}}) \rightarrow (p_T, p_T^2, 1) \right) &= \mathcal{R}_{J_q}(\mu_J \rightarrow p_T)^2 \mathcal{R}_{\mathcal{C}_q}(\mu_{\mathcal{C}_q} \rightarrow p_T)^2 \\ &\times \mathcal{R}_F^g \left((\mu_0, \zeta_{1,0}^g) \rightarrow (p_T, p_T^2) \right) \mathcal{R}_S^g \left((\mu_0, \zeta_{2,0}^{S_{\gamma q}}) \rightarrow (p_T, 1) \right),\end{aligned}\tag{5.7}$$

$$\begin{aligned}\mathcal{R}_q \left((\{\mu_k\}, \zeta_{1,0}^q, \zeta_{2,0}^{S_{\gamma q}}) \rightarrow (p_T, p_T^2, 1) \right) &= \mathcal{R}_{J_q}(\mu_J \rightarrow p_T) \mathcal{R}_{J_g}(\mu_J \rightarrow p_T) \mathcal{R}_{\mathcal{C}_q}(\mu_{\mathcal{C}_q} \rightarrow p_T) \mathcal{R}_{\mathcal{C}_g}(\mu_{\mathcal{C}_g} \rightarrow p_T) \\ &\times \mathcal{R}_F^q \left((\mu_0, \zeta_{1,0}^q) \rightarrow (p_T, p_T^2) \right) \mathcal{R}_S^g \left((\mu_0, \zeta_{2,0}^{S_{\gamma g}}) \rightarrow (p_T, 1) \right),\end{aligned}\tag{5.8}$$

where $k = \mathcal{C}_{q,g}, S_{\gamma_q, \gamma_g}, J_{q,g}$ and we have the following notation for each evolution kernel: $\mathcal{R}_{J_{f,g}}$ is the one for the jet function, $\mathcal{R}_{\mathcal{C}_{f,g}}$ is the one of collinear-soft functions, $\mathcal{R}_F^{q,g}$ the one of TMD and finally $\mathcal{R}_S^{q,g}$ is the one of the dijet soft function. Notice that in principle each evolution kernel is defined at a scale which minimizes the logs. The kernels for single-scale evolution have a standard form and a review up to NLL is given in [63],

$$\mathcal{R}_i(\mu_i \rightarrow p_T) = e^{K_i(\mu_i \rightarrow p_T)} \left(\frac{\mu_i}{m_i} \right)^{\omega_i(\mu_i \rightarrow p_T)}, \quad i = \{\mathcal{C}_q, \mathcal{C}_g, J_q, J_g\} \quad (5.9)$$

where

$$\omega_i(\mu_i \rightarrow p_T) \Big|_{\text{NLL}} = -\frac{\Gamma_i^0}{\beta_0} \left[\ln r + \left(\frac{\Gamma_1}{\Gamma_0} - \frac{\beta_1}{\beta_0} \right) \frac{\alpha_s(\mu_i)}{4\pi} (r-1) \right], \quad (5.10)$$

$$K_i(\mu_i \rightarrow p_T) \Big|_{\text{NLL}} = -\frac{\gamma_i^0}{2\beta_0} \ln r - \frac{2\pi\Gamma_i^0}{(\beta_0)^2} \left[\frac{r-1-r \ln r}{\alpha_s(p_T)} + \left(\frac{\Gamma_1}{\Gamma_0} - \frac{\beta_1}{\beta_0} \right) \frac{1-r+\ln r}{4\pi} + \frac{\beta_1}{8\pi\beta_0} \ln^2 r \right], \quad (5.11)$$

with $r = \alpha_s(p_T)/\alpha_s(\mu_i)$ and the rest of anomalous dimensions can be found in [12]. The evolution kernels for TMD, collinear-soft and soft functions resum Sudakov double logs and deserve a special discussion that we provide in the next section.

6 Evolution kernel for the soft and collinear-soft function: \mathcal{M} -scheme

The resummation of the rapidity logarithms is performed here using ζ -prescription [37]. The general form of the kernel for the functions that have both UV and rapidity evolution is

$$\mathcal{R}(\{\mu_i, \zeta_i\} \rightarrow \{\mu_f, \zeta_f\}) = \left(\frac{\zeta_f}{\zeta_i} \right)^{-\mathcal{D}(b_T; \mu_i)} \exp \left\{ \int_{\mu_i}^{\mu_f} \frac{d\bar{\mu}}{\bar{\mu}} \gamma(\alpha_s(\bar{\mu}), \zeta_f) \right\}, \quad (6.1)$$

where γ indicated the UV anomalous dimension. In the case of the ζ -prescription the TMD kernel is

$$\mathcal{R}_F^{q,g}(\{\mu_0, \zeta_0^{q,g}(b_T)\} \rightarrow \{p_T, p_T^2\}) = \left(\frac{p_T^2}{\zeta_{\mu_f}^{q,g}(b_T)} \right)^{-\mathcal{D}_{q,g}(b_T, p_T)}, \quad (6.2)$$

with $\zeta_{\mu_f}^{q,g}$ derived from the saddle point condition of the null-evolution curve, see next section and ref [37]. In ref. [12] the soft functions (S_{γ_q, γ_g}) evolution kernels have a formally similar result

$$\mathcal{R}_S^{q,g}(\{\mu_0^S, \zeta_{2,0}^{S,q,g}(b_T)\} \rightarrow \{p_T, 1\}) = \mathcal{R}_{S,(q,g)}^{c_b} \left(\frac{1}{\zeta_{2,\mu_f}^{S,q,g}(b_T)} \right)^{-\mathcal{D}_{q,g}(b_T, p_T)}, \quad (6.3)$$

and their dependence on c_b makes this direct implementation problematic. Notably, we recall that the perturbative c_b dependence in the anomalous dimensions is canceled among the soft function and the collinear-soft functions, see eq. (5.4). This cancellation is no more ensured when functions are resummed naively and spurious imaginary terms are generated. The presence of c_b dependent terms appears because of the separation of soft and collinear-soft functions and it is possibly related to a passage from SCET-II factorization to a different one, which should be further investigated. However the presence of imaginary part in the anomalous dimensions may suggest that the separation between

soft and collinear-soft functions although formally correct is not actually working. A solution for the resummation was provided in [12]. In that work all the terms that contained $c_{\mathbf{b}}$ were treated perturbatively and not resummed. At the same time the resummation involved only the part of the functions that do not depend on this angle.

In this section we start defining a different scheme that we call \mathcal{M} -scheme. The idea is to define the \mathcal{M} -functions

$$\begin{aligned}\mathcal{M}_g(\mathbf{b}_\perp, \mu, \zeta_2, R) &= C_{\bar{q}}(\mathbf{b}_\perp, R, \mu)C_q(\mathbf{b}_\perp, R, \mu)S_{\gamma_g}(\mathbf{b}_\perp, \mu, \zeta_2), \\ \mathcal{M}_q(\mathbf{b}_\perp, \mu, \zeta_2, R) &= C_g(\mathbf{b}_\perp, R, \mu)C_q(\mathbf{b}_\perp, R, \mu)S_{\gamma_q}(\mathbf{b}_\perp, \mu, \zeta_2).\end{aligned}\tag{6.4}$$

and $C_{\bar{q}} = C_q$. The respective evolution equations are

$$\begin{aligned}\frac{d}{d\ln\mu}\mathcal{M}_i &= \gamma_{\mathcal{M}_i}\mathcal{M}_i, \\ \frac{d}{d\ln\zeta}\mathcal{M}_i &= -\mathcal{D}_i\mathcal{M}_i,\end{aligned}\tag{6.5}$$

with ($i = q, \bar{q}, g$) and $\gamma_{\mathcal{M}_i}$ independent of $c_{\mathbf{b}}$,

$$\begin{aligned}\gamma_{\mathcal{M}_g}(\mu) &= 2\gamma_{C_f}(\mu, c_{\mathbf{b}}) + \gamma_{S_{\gamma_g}}(\mu, c_{\mathbf{b}}), \\ \gamma_{\mathcal{M}_q}(\mu) &= \gamma_{C_g}(\mu, c_{\mathbf{b}}) + \gamma_{C_q}(\mu, c_{\mathbf{b}}) + \gamma_{S_{\gamma_q}}(\mu, c_{\mathbf{b}}).\end{aligned}\tag{6.6}$$

Using the perturbative expansion of the anomalous dimensions

$$\gamma = \sum_{n=1} a_s^n \gamma^{[n]}, \quad \mathcal{M} = \sum_{n=1} a_s^n \mathcal{M}^{[n]}, \quad a_s = \frac{\alpha_s}{4\pi},\tag{6.7}$$

the one loop expression of $\gamma_{\mathcal{M}_i}$ are

$$\begin{aligned}\gamma_{\mathcal{M}_g}^{[1]} &= -4C_A \ln\zeta_2 - 8C_F \ln\frac{\hat{s}}{p_T^2 R^2}, \\ \gamma_{\mathcal{M}_q}^{[1]} &= -4(C_F + C_A) \ln\frac{\hat{s}}{p_T^2 R^2} + 4(C_F - C_A) \ln\left(\frac{\hat{t}}{\hat{u}}\right) - 4C_F \ln\zeta_2.\end{aligned}\tag{6.8}$$

Notably, this structure exhibits no angular dependence and one can use standard ζ -prescription rules to evolve this function so that one obtains

$$\mathcal{R}_{\mathcal{M}_{q,g}}(\{\mu_0, \zeta_{2,0}^{\mathcal{M}_{q,g}}(b)\} \rightarrow \{p_T, 1\}) = \left(\frac{1}{\zeta_{2,\mu_f}^{\mathcal{M}_{q,g}}(b)} \right)^{-\mathcal{D}_{q,g}(b,p_T)}\tag{6.9}$$

as the evolution kernel from the saddle point $(\mu_0, \zeta_{2,0}^{\mathcal{M}})$ to the highest scales $(p_T, 1)$.

6.1 Scale fixing and non-perturbative effects

The TMD evolution is fundamental for the predictions and the ζ -prescription, which is already included in the code `artemide`, was used to fit the quark Sivers function [44, 64]. The TMD evolution kernel \mathcal{D} has been object of many phenomenological researches in refs. [43](ART25), [42] (ART23), [41] (SV19), [65] (MAPNN), [47] (MAP24) and [45] (MAP22); lattice computations performed in refs. [66] (BGMZ24), [67, 68] (ASWZ24), [69] (SSSV23), [70] (LPC22); parton branching within the

CASCADE generator [71, 72] determined by the method of ref. [73]; instanton vacuum model [74], thrust distributions in single inclusive electron-positron annihilation data in ref. [75], and hadron-structure oriented approach [76].

In the cross section of the dijet system we have functions with single (μ) and double scale (μ, ζ) evolution. For practical implementation we need to discuss the proper scale at which each function is initially defined.

The simplest object to treat is the single scale dependent jet functions $J_{f,\bar{f},g}$. For that we evolve from $\mu_J = p_T R$ to the high scale p_T . For our EIC predictions of this work we use

$$p_T = 20 \text{ GeV}, \quad R = 0.7, \quad (6.10)$$

The double scale evolution is instead more complicated and also the usage of ζ -prescription is not unique. We show here two possible example of definition of this prescription which are related to the complication provided by the c_b dependence of some of the anomalous dimensions as discussed in sec. 5. In [12] the evolution of each function was performed with the initial and final scale choices

$$\mathcal{R}_{\mathcal{C}_{q,g}} : \mu_{\mathcal{C}_q} = \mu_{\mathcal{C}_g} = 2e^{-\gamma_E} \left(\frac{1}{b_T} + \frac{1}{b_{\max}^c} \right) \longrightarrow p_T, \quad (6.11)$$

$$\mathcal{R}_{\mathcal{S}_{\gamma q}}, \mathcal{R}_{\mathcal{S}_{\gamma g}} : (\mu_0, \zeta_{2,0}^{S_{q,g}}(b)) = \left(\frac{2e^{-\gamma_E}}{b^*}, \zeta_{2,0}^{S_{q,g}}(b) \right) \longrightarrow (p_T, 1), \quad (6.12)$$

$$\mathcal{R}_{F_{q,g}} : (\mu_0, \zeta_{1,0}^{(\gamma^i),(\gamma^g)}(b)) = \left(\frac{2e^{-\gamma_E}}{b^*}, \zeta_{1,0}^{(\gamma^i),(\gamma^g)}(b) \right) \longrightarrow (p_T, p_T^2), \quad (6.13)$$

with

$$b^* = \frac{b_T}{\sqrt{1 + b_T^2/b_{\max}^2}}, \quad (6.14)$$

and the values of the constants are in tab. 1².

	$\{\mathcal{C}_i, \mathcal{S}_{\gamma i}, \mathcal{M}_i\}$ eq. (6.15), (6.22)		$\{\mathcal{C}_i, \mathcal{S}_{\gamma i}, \mathcal{M}_i\}$ eq. (6.14)
β_{NP} (GeV ⁻¹)	2.5	b_{\max} (GeV ⁻¹)	2.5

Table 1: Values of non-perturbative parameter B_{NP} and b_{\max} prescription chosen for collinear-soft, dijet soft and \mathcal{M} -functions (see also footnote 2). Indices $i = q, \bar{q}, g$.

A first solution for ζ -prescription was also provided in the same work. The values of $\zeta_{1,0}$ and $\zeta_{2,0}$ have been calculated perturbatively and in exact form in [37, 41, 77] and [11] respectively. The expression for ζ_{2,μ_f} is

$$\zeta_{2,\mu_f}^{S_{q,g}}(b_T) = \zeta_{2,\mu_f}^{S_{q,g}\text{pert}} e^{-b_T^2/B_\zeta^2} + \zeta_{2,\mu_f}^{S_{q,g}\text{exact}} (1 - e^{-b_T^2/B_\zeta^2}) \quad (6.15)$$

with $B_\zeta = 0.01 \text{ GeV}^{-1}$ in ART23/ART25 and $B_\zeta = 1 \text{ GeV}^{-1}$ in [12]. In this work we use $B_\zeta = 0.01 \text{ GeV}^{-1}$ for consistency with more modern versions of the code ART23 and ART25. Because in the cross section we have the product of 2 collinear-soft and one dijet soft functions treated independently we refer to this way to implement the ζ -prescription and "CCS-scheme".

²In principle one can choose a different b_{\max} or B_{NP} for each function, but in our analysis we finally opted for a single common value.

Despite the fact that in CCS scheme the logs are resummed in each function separately, in practice the angular c_b dependence of the collinear-soft and soft anomalous dimensions creates problems. As noticed in [12] only angular c_b -independent parts of the anomalous dimensions can be resummed while for the rest one relies on a perturbative treatment. Moreover the interval of possible μ -scale values is limited in order not to spoil mathematical consistency.

An alternative approach that we follow here uses the \mathcal{M} -function introduced in sec. 5. This consists in calculating the special initial saddle point scales of ζ -prescription for the \mathcal{M} -function. They are define by $(\mu_0, \zeta_{2,0}^{\mathcal{M}})$ such that,

$$\mathcal{D}_i(\mu_0(b_T), b_T) = 0, \quad \gamma_{\mathcal{M}_i}(\mu_0(b_T), \zeta_{2,0}^{\mathcal{M}_i}(b_T)) = 0, \quad \text{with } i = q, g. \quad (6.16)$$

To obtain the value of $\zeta_{2,0}^{\mathcal{M}}$ perturbatively at one loop we start from the definition of the anomalous dimension of the total soft function for the gluon and quark channels in eq. (6.8),

$$\begin{aligned} \gamma_{\mathcal{M}_g}^{[1]} &= -4C_A \ln \frac{\zeta_2}{\zeta_{2,0}^{\mathcal{M}_g}}, \\ \gamma_{\mathcal{M}_q}^{[1]} &= -4C_F \ln \frac{\zeta_2}{\zeta_{2,0}^{\mathcal{M}_q}}, \end{aligned} \quad (6.17)$$

where we have put

$$\begin{aligned} \zeta_{2,0}^{\mathcal{M}_q} &= \left(\frac{p_T^2 R^2}{\hat{s}} \right)^{\frac{C_F+C_A}{C_F}} \left(\frac{\hat{t}}{\hat{u}} \right)^{\frac{C_F-C_A}{C_F}}, \\ \zeta_{2,0}^{\mathcal{M}_g} &= \left(\frac{p_T^2 R^2}{\hat{s}} \right)^{2\frac{C_F}{C_A}}. \end{aligned} \quad (6.18)$$

The evolution kernel of the total function \mathcal{M} using the ζ prescription is then given by:

$$\mathcal{R}_{\mathcal{M}_{q,g}} : (\mu_0, \zeta_{2,0}^{\mathcal{M}_{q,g}}(b_T)) = \left(\frac{2e^{-\gamma_E}}{b^*}, \zeta_{2,0}^{\mathcal{M}_{q,g}}(b_T) \right) \longrightarrow (p_T, 1), \quad (6.19)$$

and the problem of angular dependence in the anomalous dimension disappears.

In the \mathcal{M} function the angular dependence is by definition only present at the initial scale where this function is perturbatively evaluated and the results at one loop are shown in the next-section.

In the proposed factorization it is necessary to introduce non-perturbative effects. In CCS-scheme we need to specify a nonperturbative part for collinear-soft and dijet soft functions

$$\begin{aligned} \mathcal{C}_i(b_T, R; p_T) &= \mathcal{R}_{\mathcal{C}_i}(b^*, \mu_{\mathcal{C}_i} \rightarrow p_T) \mathcal{C}_i^{pert}(b^*, R; \mu_{\mathcal{C}_i}) f_{\mathcal{C}_i}^{\text{NP}}(b_T), \\ S_{\gamma_i}(b_T; p_T, 1) &= \mathcal{R}_{S_i}(b^*, \{\mu_0, \zeta_{2,0}^{\gamma_i}\} \rightarrow \{p_T, 1\}) S_{\gamma_i}^{pert}(b^*; \mu_0, \zeta_{2,0}^{\gamma_i}) f_{S_i}^{\text{NP}}(b_T), \quad (\text{with } i = q, g), \end{aligned} \quad (6.20)$$

where the functions with label *pert* are their perturbative part in the $\overline{\text{MS}}$ scheme, currently known at one loop.

The \mathcal{M} -scheme needs a different set of nonperturbative parameters, namely

$$\mathcal{M}_i(b_T, R; p_T, 1) = \mathcal{R}_{\mathcal{M}_i}(b^*, \{\mu_0, \zeta_{2,0}^{\mathcal{M}_i}\} \rightarrow \{p_T, 1\}) \mathcal{M}_i^{pert}(b^*, R; \mu_0, \zeta_{2,0}^{\mathcal{M}_i}) f_{\mathcal{M}_i}^{\text{NP}}(b_T), \quad i = q, g. \quad (6.21)$$

The non-perturbative model is given by

$$f_i^{\text{NP}}(b_T) = \exp \left(- \frac{b_T^2}{(\beta_{\text{NP}}^i)^2} \right), \quad i = \mathcal{C}_{q,g}, \mathcal{M}_{q,g}, S_{\gamma q, \gamma g}. \quad (6.22)$$

The values of β_{NP}^i determine the non-perturbative model. Assuming that most of the contribution is of perturbative origin the values of β_{NP}^i should be around 1-3 GeV⁻¹. We have finally made the choice of tab. 1 to provide numerical results.

6.2 Final expression of the unpolarized hadronic tensor

Using the \mathcal{M} -scheme the hadronic tensor contributions are respectively

$$\begin{aligned}
W_g^{UU} &= r_T \sigma_0^{fU} \sum_{q=\text{flav.}} H_{\gamma^* g \rightarrow q \bar{q}}^U(\hat{s}, \hat{t}, \hat{u}, \mu) \int \frac{b_T db_T}{(2\pi)} J_0(r_T b_T) J_{\bar{q}}(p_T, R, \mu_{J_{\bar{q}}}) J_q(p_T, R, \mu_{J_q}) f_1^g(\xi, b_T) \\
&\times \mathcal{R}_F^g(\{\mu_0, \zeta_{1,0}^g\} \rightarrow \{p_T, p_T^2\}) \mathcal{R}_{\mathcal{M}_g}(\{\mu_0, \zeta_{2,0}^{\mathcal{M}_g}\} \rightarrow \{p_T, 1\}) \mathcal{R}_{J_{\bar{q}}}(\mu_{J_{\bar{q}}} \rightarrow p_T) \mathcal{R}_{J_q}(\mu_{J_q} \rightarrow p_T) \\
&\times \int_{-\pi}^{\pi} d\phi_b \mathcal{M}_g(\mathbf{b}_{\perp}, R, \zeta_{2,0}^{\mathcal{M}_g}, \mu_0), \tag{6.23}
\end{aligned}$$

$$\begin{aligned}
W_q^{UU} &= r_T \sigma_0^{fU} H_{\gamma^* q \rightarrow g q}^U(\hat{s}, \hat{t}, \hat{u}, \mu) \int \frac{b_T db_T}{(2\pi)} J_0(r_T b_T) J_g(p_T, R, \mu_{J_g}) J_q(p_T, R, \mu_{J_q}) f_1(\xi, b_T) \\
&\times \mathcal{R}_F^q(\{\mu_0, \zeta_{1,0}^q\} \rightarrow \{p_T, p_T^2\}) \mathcal{R}_{\mathcal{M}_q}(\{\mu_0, \zeta_{2,0}^{S_q}\} \rightarrow \{p_T, 1\}) \mathcal{R}_{J_g}(\mu_{J_g} \rightarrow p_T) \mathcal{R}_{J_q}(\mu_{J_q} \rightarrow p_T) \\
&\times \int_{-\pi}^{\pi} d\phi_b \mathcal{M}_q(\mathbf{b}_{\perp}, R, \zeta_{2,0}^{\mathcal{M}_q}, \mu_0), \tag{6.24}
\end{aligned}$$

where J_0 is the Bessel function and similarly one can define $W_{\bar{q}}^{UU}$ interchanging $q \leftrightarrow \bar{q}$. If one follows the scale fixing according the work [12] the evolution factors of the collinear-soft and dijet soft functions have angular dependence and the formulas of the hadronic tensor change. Using eq. (5.7-5.8) one writes

$$\begin{aligned}
W_g^{UU} &= r_T \sigma_0^{fU} \sum_{q=\text{flav.}} H_{\gamma^* g \rightarrow q \bar{q}}^U(\hat{s}, \hat{t}, \hat{u}, \mu) \int \frac{b_T db_T}{(2\pi)} J_0(r_T b_T) J_{\bar{q}}(p_T, R, \mu_{J_{\bar{q}}}) J_q(p_T, R, \mu_{J_q}) f_1^g(\xi, b_T) \\
&\times \int_{-\pi}^{\pi} d\phi_b \mathcal{R}_g(\{(\mu_k), \zeta_{1,0}^g, \zeta_{2,0}^{S_{\gamma q}}\} \rightarrow (p_T, p_T^2, 1)) \\
&\times \mathcal{C}_{\bar{q}}(\mathbf{b}_{\perp}, R, \mu_{C_{\bar{q}}}) \mathcal{C}_q(\mathbf{b}_{\perp}, R, \mu_{C_q}) \mathcal{S}_{\gamma g}(\mathbf{b}_{\perp}, \zeta_{2,0}^{S_g}, \mu_0) \tag{6.25}
\end{aligned}$$

$$\begin{aligned}
W_q^{UU} &= r_T \sigma_0^{fU} H_{\gamma^* q \rightarrow g q}^U(\hat{s}, \hat{t}, \hat{u}, \mu) \int \frac{b_T db_T}{(2\pi)} J_0(r_T b_T) J_g(p_T, R, \mu_{J_g}) J_q(p_T, R, \mu_{J_q}) f_1(\xi, b_T) \\
&\times \int_{-\pi}^{\pi} d\phi_b \mathcal{R}_q(\{(\mu_k), \zeta_{1,0}^q, \zeta_{2,0}^{S_{\gamma q}}\} \rightarrow (p_T, p_T^2, 1)) \\
&\times \mathcal{C}_g(\mathbf{b}_{\perp}, R, \mu_{C_g}) \mathcal{C}_i(\mathbf{b}_{\perp}, R, \mu_{C_q}) \mathcal{S}_{\gamma q}(\mathbf{b}_{\perp}, \zeta_{2,0}^{S_q}, \mu_0), \tag{6.26}
\end{aligned}$$

and the angular integration includes also the evolution factors.

6.3 Final expression of the hadronic tensor for Sivers function measurement

The general expression for the hadronic tensor has been given in formula (3.24) without specifying the evolution of the distributions that compose it. For the case in which we use the \mathcal{M} -scheme we

have

$$\begin{aligned}
W_g^{UT} &= -r_T S_T \sigma_0^{fU} \sum_{q=\text{flav.}} H_{\gamma^* g \rightarrow q\bar{q}}^U(\hat{s}, \hat{t}, \hat{u}, \mu) \int \frac{b_T db_T}{(2\pi)} J_1(r_T b_T) J_{\bar{q}}(p_T, R, \mu_{J_{\bar{q}}}) J_q(p_T, R, \mu_{J_q}) (b_T M) f_{1T}^{\perp g}(\xi, b) \\
&\times \mathcal{R}_F^g(\{\mu_0, \zeta_{1,0}^g\} \rightarrow \{p_T, p_T^2\}) \mathcal{R}_{\mathcal{M}_g}(\{\mu_0, \zeta_{2,0}^{\mathcal{M}_g}\} \rightarrow \{p_T, p_T^2\}) \mathcal{R}_{J_{\bar{q}}}(\mu_{J_{\bar{q}}} \rightarrow p_T) \mathcal{R}_{J_q}(\mu_{J_q} \rightarrow p_T) \\
&\times \int_{-\pi}^{\pi} d\phi_b \sin^2(\phi_S - \phi_b) \mathcal{M}_g(\mathbf{b}_{\perp}, R, \zeta_0^{S_g}, \mu_0), \tag{6.27}
\end{aligned}$$

$$\begin{aligned}
W_q^{UT} &= -r_T S_T \sigma_0^{fU} H_{\gamma^* q \rightarrow gq}^U(\hat{s}, \hat{t}, \hat{u}, \mu) \int \frac{b_T db_T}{(2\pi)} J_1(r_T b_T) J_g(p_T, R, \mu_{J_g}) J_q(p_T, R, \mu_{J_q}) (b_T M) f_{1T}^{\perp}(\xi, b_T) \\
&\times \mathcal{R}_F^q(\{\mu_0, \zeta_{1,0}^q\} \rightarrow \{p_T, p_T^2\}) \mathcal{R}_{\mathcal{M}_q}(\{\mu_0, \zeta_0^{S_q}\} \rightarrow \{p_T, p_T^2\}) \mathcal{R}_{J_g}(\mu_{J_g} \rightarrow p_T) \mathcal{R}_{J_q}(\mu_{J_q} \rightarrow p_T) \\
&\times \int_{-\pi}^{\pi} d\phi_b \sin^2(\phi_S - \phi_b) \mathcal{M}_q(\mathbf{b}_{\perp}, R, \zeta_0^{S_q}, \mu_0), \tag{6.28}
\end{aligned}$$

and the expression holds for $W_{\bar{q}}^{UT}$ with the interchange $q \leftrightarrow \bar{q}$. For completeness we provide the one-loop expression for \mathcal{M} function in the next section.

If one follows the scale fixing according the work [12] the evolution factors of the CCS-scheme have angular dependence and the formulas of the hadronic tensor change to

$$\begin{aligned}
W_g^{UT} &= -r_T S_T \sigma_0^{fU} \sum_{q=\text{flav.}} H_{\gamma^* g \rightarrow q\bar{q}}^U(\hat{s}, \hat{t}, \hat{u}, \mu) \int \frac{b_T db_T}{(2\pi)} J_1(r_T b_T) J_{\bar{q}}(p_T, R, \mu_{J_{\bar{q}}}) J_q(p_T, R, \mu_{J_q}) (b_T M) f_1^{g\perp}(\xi, b_T) \\
&\times \int_{-\pi}^{\pi} d\phi_b \sin^2(\phi_S - \phi_b) \mathcal{R}_g\left(\left(\{\mu_k\}, \zeta_{1,0}^g, \zeta_{2,0}^{S_{\gamma q}}\right) \rightarrow (p_T, p_T^2, 1)\right) \\
&\times \mathcal{C}_{\bar{q}}(\mathbf{b}_{\perp}, R, \mu_{\mathcal{C}_{\bar{q}}}) \mathcal{C}_q(\mathbf{b}_{\perp}, R, \mu_{\mathcal{C}_q}) \mathcal{S}_{\gamma g}(\mathbf{b}_{\perp}, \zeta_{2,0}^{S_g}, \mu_0) \tag{6.29}
\end{aligned}$$

$$\begin{aligned}
W_q^{UT} &= -r_T S_T \sigma_0^{fU} \sum_{q=\text{flav.}} H_{\gamma^* q \rightarrow gq}^U(\hat{s}, \hat{t}, \hat{u}, \mu) \int \frac{b_T db_T}{(2\pi)} J_0(r_T b_T) J_g(p_T, R, \mu_{J_g}) J_q(p_T, R, \mu_{J_q}) (b_T M) f_1^{\perp}(\xi, b_T) \\
&\times \int_{-\pi}^{\pi} d\phi_b \sin^2(\phi_S - \phi_b) \mathcal{R}_q\left(\left(\{\mu_k\}, \zeta_{1,0}^q, \zeta_{2,0}^{S_{\gamma q}}\right) \rightarrow (p_T, p_T^2, 1)\right) \\
&\times \mathcal{C}_g(\mathbf{b}_{\perp}, R, \mu_{\mathcal{C}_g}) \mathcal{C}_i(\mathbf{b}_{\perp}, R, \mu_{\mathcal{C}_q}) \mathcal{S}_{\gamma q}(\mathbf{b}_{\perp}, \zeta_{2,0}^{S_{\gamma q}}, \mu_0), \tag{6.30}
\end{aligned}$$

the angular integration includes also the evolution factors and we have used eq. (5.7-5.8). As in the unpolarized case in the latter formulas the resummation of different functions is fixed with a different choice of scales, which minimizes the logs of each function separately.

6.4 \mathcal{M} -function scheme at one loop

In this section we collect the relevant one-loop expressions for the \mathcal{M} -function. Using the notation of eq. (6.7) At one loop we have

$$\mathcal{M}_g(\mathbf{b}_{\perp}, \mu, \zeta_2, R)^{[1]} = \mathcal{C}_{\bar{q}}(\mathbf{b}_{\perp}, R, \mu)^{[1]} + \mathcal{C}_q(\mathbf{b}_{\perp}, R, \mu)^{[1]} + \mathcal{S}_{\gamma g}(\mathbf{b}_{\perp}, \mu, \zeta_2)^{[1]} \tag{6.31}$$

$$\mathcal{M}_q(\mathbf{b}_{\perp}, \mu, \zeta_2, R)^{[1]} = \mathcal{C}_g(\mathbf{b}_{\perp}, R, \mu)^{[1]} + \mathcal{C}_q(\mathbf{b}_{\perp}, R, \mu)^{[1]} + \mathcal{S}_{\gamma, f}(\mathbf{b}_{\perp}, \mu, \zeta_2)^{[1]} \tag{6.32}$$

where on the r.h.s. we indicate the one-loop expression for all these functions. Combining the results of previous calculations we have

$$\mathcal{M}_g^{[0]}(\mathbf{b}, R, \mu, \zeta) = 1, \quad (6.33)$$

$$\begin{aligned} \mathcal{M}_g^{[1]}(\mathbf{b}, R, \mu, \zeta) &= a_s \left\{ C_F \left[\frac{\pi^2}{3} + 2 \ln^2 \left(\frac{B e^{2\gamma_E} \mu^2}{-A_{\mathbf{b}}} \right) + 4 \text{Li}_2(1 + A_{\mathbf{b}}) \right] \right. \\ &\quad \left. + C_A \left[-2 \ln(B e^{2\gamma_E} \mu^2) \ln \zeta - \ln^2(-A_{\mathbf{b}}) - \frac{\pi^2}{3} - 2 \text{Li}_2(1 + A_{\mathbf{b}}) \right] \right\} \\ &\quad - 8 a_s C_F \left[\ln^2 \left(\frac{\mu e^{\gamma_E} b}{R} \right) + \frac{\pi^2}{8} + \ln^2(-i \cos \phi_b) + 2 \ln \left(\frac{\mu e^{\gamma_E} b}{R} \right) \ln(-i \cos \phi_b) \right] + \mathcal{O}(a_s^2), \end{aligned} \quad (6.34)$$

for gluons and

$$\mathcal{M}_q^{[0]}(\mathbf{b}_\perp, R, \mu, \zeta_2) = 1, \quad (6.35)$$

$$\begin{aligned} \mathcal{M}_q^{[1]}(\mathbf{b}_\perp, R, \mu, \zeta_2) &= a_s \left\{ C_A \left[\frac{\pi^2}{6} + \ln^2 \left(\frac{B \mu^2 e^{2\gamma_E}}{-A_{\mathbf{b}_\perp}} \right) + 2 \text{Li}_2(1 + A_{\mathbf{b}_\perp}) + 2 \ln(B \mu^2 e^{2\gamma_E}) \ln \frac{(n \cdot v_1)(\mathbf{v}_2 \cdot \mathbf{b}_\perp)}{(n \cdot v_2)(\mathbf{v}_1 \cdot \mathbf{b}_\perp)} \right] \right. \\ &\quad \left. + C_F \ln(B \mu^2 e^{2\gamma_E}) \left[\ln(B \mu^2 e^{2\gamma_E}) - 2 \ln \zeta_2 + 2 \ln \left(\frac{2(n \cdot v_2)}{(v_1 \cdot v_2)(n \cdot v_2)} \right) - \frac{\pi^2}{6} + 4 \ln(-i \mathbf{v}_1 \cdot \hat{\mathbf{b}}_\perp) \right] \right\} \\ &\quad - 4 a_s (C_A + C_F) \left[\ln^2 \left(\frac{\mu e^{\gamma_E} b}{R} \right) + \frac{\pi^2}{8} + \ln^2(-i \cos \phi_b) + 2 \ln \left(\frac{\mu e^{\gamma_E} b}{R} \right) \ln(-i \cos \phi_b) \right], \end{aligned} \quad (6.36)$$

for quarks. In the hadronic tensor these expressions are angularly integrated providing

$$\begin{aligned} &\int_{-\pi}^{\pi} d\phi_b \sin^2(\phi_S - \phi_b) \mathcal{M}_g^{[1]}(\mathbf{b}_\perp, R, \mu, \zeta) \\ &= a_s \left\{ C_F \left[\frac{\pi^3}{3} + 2\pi \ln^2(B \mu^2 e^{2\gamma_E}) + 2 I_{A_b^2} - 4 \ln(B \mu^2 e^{2\gamma_E}) I_{A_b} + 4 I_{Li_2} \right] \right. \\ &\quad \left. + C_A \left[-2\pi \ln(B \mu^2 e^{2\gamma_E}) \ln \zeta - I_{A_b^2} - \frac{\pi^3}{3} - 2 I_{Li_2} \right] \right\} \\ &\quad - 8 a_s C_F \left[\pi \ln^2 \left(\frac{\mu e^{\gamma_E} b}{R} \right) + \frac{\pi^3}{8} + 2 \ln \left(\frac{\mu e^{\gamma_E} b}{R} \right) I_{log} + I_{log^2} \right], \end{aligned} \quad (6.37)$$

for gluons and

$$\begin{aligned}
\int_{-\pi}^{\pi} d\phi_b \sin^2(\phi_S - \phi_b) \mathcal{M}_f^{[1]}(\mathbf{b}_\perp, \mu, \zeta_2, R) = a_s \left\{ C_A \left[\frac{\pi^3}{6} + \pi \ln^2(B\mu^2 e^{2\gamma_E}) + I_{A_b^2} \right. \right. \\
- 2 \ln(B\mu^2 e^{2\gamma_E}) I_{A_b} + 2 I_{Li_2} + 2 \ln(B\mu^2 e^{2\gamma_E}) \ln \frac{t}{u} \left(-\cos 2\phi_S I_0(1) + \cos^2 \phi_S I_0(0) \right) \Big] \\
+ C_F \ln(B\mu^2 e^{2\gamma_E}) \left[\pi \ln(B\mu^2 e^{2\gamma_E}) - 2\pi \ln \zeta_2 - \frac{\pi^3}{6} \right. \\
- 2 \cos 2\phi_S \ln \frac{t}{u} I_0(1) + 2 \cos^2 \phi_S \ln \frac{t}{u} I_0(0) - 2 I_{A_b} \Big] \Big\} \\
- 4 a_s (C_A + C_F) \left[\pi \ln^2 \left(\frac{\mu e^{\gamma_E} b}{R} \right) + \frac{\pi^3}{8} + 2 \ln \left(\frac{\mu e^{\gamma_E} b}{R} \right) I_{log} + I_{log^2} \right], \tag{6.38}
\end{aligned}$$

for quarks. The explicit expression for the terms in these equations is provided in the appendix.

7 The quark and gluon CS-kernels for evolution

In the ART23/ART25 extractions of unpolarized TMD the the evolution (CS) kernel has the general form

$$\mathcal{D}_{q,g}(b_T, \mu) = \mathcal{D}_{q,g,\text{pert}}(b^*, \mu^*) + \int_{\mu_{q,g}^*}^{\mu} \frac{d\mu'}{\mu'} \Gamma_{\text{cusp}}(\mu') + \mathcal{D}_{q,g,\text{NP}}(b_T), \tag{7.1}$$

where b^* ,

$$b_{q,g}^*(b_T) = \frac{b_T}{\sqrt{1 + \frac{b_T^2}{(B_{\text{NP}}^{q,g})^2}}}, \quad \mu_{q,g}^*(b_T) = 2 \exp^{-\gamma_E} / b_{q,g}^*(b_T), \tag{7.2}$$

and B_{NP} 's for the kernels take a value as in tab. 2,

$\mathcal{D}_{\text{pert}}$'s are the perturbative expression of the kernel at N³LO [78, 79], and \mathcal{D}_{NP} 's are the non-perturbative parts to be modeled. Up to three loops we have $\mathcal{D}_{\text{pert}}^q = (C_F/C_A) \mathcal{D}_{\text{pert}}^g$ and $\Gamma_{\text{cusp}}^q = (C_F/C_A) \Gamma_{\text{cusp}}^g$ and differences appear at 4 loops. The integral term in eq. (7.1) describes the evolution from the scale μ_q^* to μ . For the quark case we have

$$\mathcal{D}_{\text{NP}}^q(b_T) = b_T b^* \left[c_0 + c_1 \ln \left(\frac{b^*}{B_{\text{NP}}^q} \right) \right], \tag{7.3}$$

with c_0 and c_1 free parameters. At large- b_T the b^* prescription freezes at $b_T \sim B_{\text{NP}}^q$ preventing the approaching to the Landau pole of the perturbative part. and the kernel is dominated by \mathcal{D}_{NP} . The two fits use different sets of data and the phenomenologically extracted parameters have some tension between each other, as one can see in tab. 2.

The evolution kernel values are however different for quark and gluon cases so that we have to distinguish \mathcal{D}^q and \mathcal{D}^g . In ART23/ART25 it was implemented also $\mathcal{D}_{\text{NP}}^q = \mathcal{D}_{\text{NP}}^g$ while here we prefer to set $\mathcal{D}_{\text{NP}}^q = (C_F/C_A) \mathcal{D}_{\text{NP}}^g$. The fits however are not very sensitive to the gluon nonperturbative parts (in fact they use DY and SIDIS data which are dominated by quark channels).

As a matter of fact we find a great sensitivity to both quark and gluon evolution kernels. In \mathcal{M} -scheme we use the same values of B_{NP} as in the original codes. In CCS-scheme instead we have less convergence and we choose the evolution kernel parameters $B_{\text{NP}}^q = B_{\text{NP}}^g = 1 \text{ GeV}^{-1}$. In CCS-scheme, we also need to improve the numerical stability by freezing the value of \mathcal{D}_{NP} at $b = 6 \text{ GeV}^{-1}$.

Parameter	ART25	ART23
c_0 (GeV ⁻²)	$0.0859^{+0.0023}_{-0.0017}$	$0.0369^{+0.0065}_{-0.0061}$
c_1 (GeV ⁻²)	$0.0303^{0.0038}_{-0.0041}$	$0.0582^{+0.0064}_{-0.0088}$
$B_{NP}^q = B_{NP}^g$ (GeV ⁻¹)	1.5 (fixed,[43])	$1.56^{+0.013}_{-0.09}$ [42]

Table 2: Parameters for the nonperturbative part of the Collins-Soper kernel, \mathcal{D}_{NP} in ART25/ART23. See discussion in the sec. 7 .

8 Sivers function models

In the past, several models for Sivers functions have been proposed for the quark distributions [44, 64, 80, 81], while there are less studies for the gluon functions [82]. A comparison among models is difficult because of the methodology of evolution used in each work which is recapitulated in tab. 3. The main differences come from the inclusion of the evolution and TMD fragmentation functions in the analysis of SIDIS data. TMD evolution factors usually provide a suppression of the cross section. In cases where this is not included the Sivers distributions are much suppressed. In the

Reference	TMD Evolution kernel
[81]	none
[80]	NNLL (Collins like)
[44, 64]	N3LO (<i>artemide</i>)

Table 3: Some models for extracted Sivers function and main features of the fits

present work we adopted the model and the parameters for the quark Sivers function of ref. [44] as default. This model has been tested in [44] to substantially agree with the one in [80]. There is no direct extraction of the Sivers gluon function up to now so that some ansatz must be provided. In the extraction [44, 64] the flavor dependence is partially included and light quarks are distinguished from the sea. We consider the gluon contribution as part of the sea for those cases, so that for the Sivers gluon function we use as default the same model as for the sea case in [44]. In the next section we also study different normalization of this model in order to provide a discussion about this ansatz. Here we provide some information about the quark models in ref. [44]. A summary of the model in [80] is reported in the appendix E.

8.1 Models for quark Sivers function

By comparison with models of ref. [44] (BPV) and ref. [80] (EKT) we obtain

$$f_{1T}^\perp(\xi, b_T) = f_{1T, \text{BPV}}^\perp(\xi, b_T) = f_{1T, \text{EKT}}^\perp(\xi, b_T). \quad (8.1)$$

where in the l.h.s we have our definition.

8.1.1 Model BPV

In [44] the authors consider the Sivers function as a generic non-perturbative function that is extracted from the data. The resulting definition is:

$$f_{1T,\text{BPV}}^\perp(\xi, b_T) = N_q \frac{(1-x)x^{\beta_q}(1+\epsilon_q x)}{n(\beta_q, \epsilon_q)} \exp\left(-\frac{r_0 + xr_1}{\sqrt{1+r_2 x^2 b_T^2}} b_T^2\right), \quad (8.2)$$

where $n(\beta, \epsilon) = (3 + \beta + \epsilon + \epsilon\beta)\Gamma(\beta + 1)/\Gamma(\beta + 4)$, such that

$$\int_0^1 dx f_{1T,\text{BPV}}^\perp(\xi, 0) = N_q. \quad (8.3)$$

The factor in front of the exponential is independent of the transverse variable b_T and parametrizes the Qiu-Sterman function to be obtained in the limit $b_T \rightarrow 0$. The values obtained for the parameters in the fit are reported in appendix D table 4.

9 Results

The results presented in this work correspond to the cross section defined in eq. (3.25), evaluated at central rapidity $\eta^\pm = 0$ using eq. (3.22) and $p_T^0 = 20$ GeV. For central rapidity we have $x \in (0.0859, 0.5)$ which corresponds to the inelasticity interval $y \in (0.16, 0.95)$. We use ART25 [43] settings as default. Following the discussion in the previous sections, we present predictions in two renormalization schemes: one based on the \mathcal{M} function (hereafter referred to as the \mathcal{M} scheme), and another in which the \mathcal{M} function is further factorized into collinear-soft and soft functions (the CCS scheme). The unpolarized dijet cross sections obtained in the two schemes are shown in Fig. 3. The CCS scheme was previously employed in [12]. After revisiting the numerical implementation used in that analysis, we identified and corrected sign inconsistencies; however, the overall conclusions remain consistent with those reported there.

The two schemes lead to compatible predictions for the central values of the distributions, and the relative contributions from quark and gluon channels are found to be consistent. The uncertainty bands shown in the figures are obtained from variations of the hard scale and represent the dominant perturbative uncertainty, in agreement with [12]. The uncertainty is larger in the CCS scheme than in the \mathcal{M} scheme, which we interpret as an indication of improved perturbative stability in the latter. The comparison of the final cross sections obtained in the two schemes is displayed on the right-hand side of Fig. 3. Similar observations are true for the polarized cross sections shown in fig. 4. In this case quark and gluon distributions contribute almost equally to the cross section for the CCS-scheme, while their separate contribution is different in the case of the \mathcal{M} -scheme. The two schemes however agree within errors and the final result of the polarized cross section are compared on r.h.s of fig. 4 with bands corresponding to hard scale errors.

The Sivers asymmetry is then shown in fig. 5 with the two renormalization schemes and hard scale error bands. We have estimated the model error using the bootstrap method and 500 replicas extracted from ref. [44]. As expected the errors are very big and the relative bands are shown in fig. 6 with the two renormalization schemes. The corresponding final results for the Sivers asymmetry is in fig. 7. The asymmetry can be large, having its peak for $r_T \sim 1\text{-}2$ GeV with a value in the interval 5-50%.

We have compared the predictions for the Sivers asymmetry obtained using the evolution kernels and distributions from the ART23 [42] and ART25 [43] analyses. The \mathcal{M} scheme exhibits a stronger

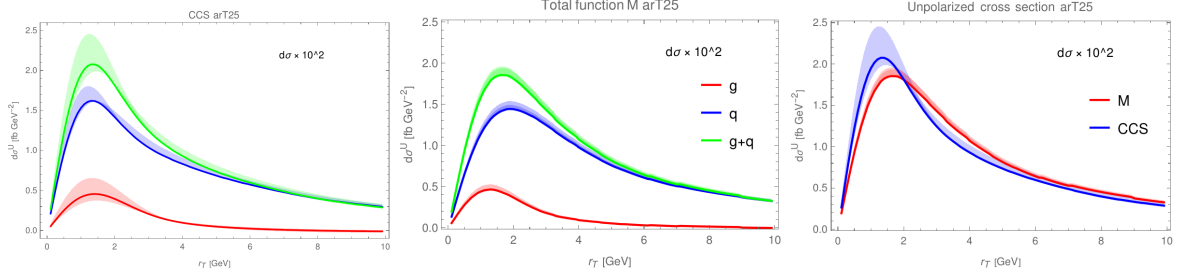


Figure 3: Unpolarized cross-section using CCS-scheme (left) and \mathcal{M} -scheme. (center). We show separately gluon-channel (red), quark-channel contributions and final result (green). In the left plot we show the comparison of unpolarized cross-section in \mathcal{M} - and CCS-schemes, respectively, in red and blues lines. The band corresponds to hard function uncertainty.

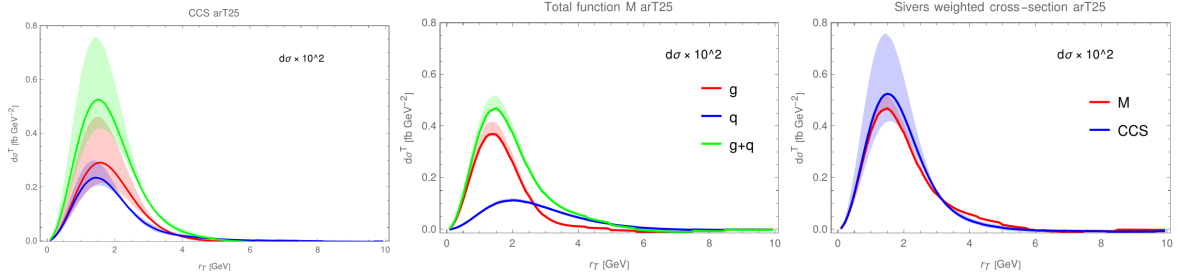


Figure 4: Siivers weighted cross-section using CCS-scheme (left) and \mathcal{M} -scheme. (center). We show separately gluon-channel (red), quark-channel contributions and final result (green). In the left plot we show the comparison of Siivers weighted cross-section in \mathcal{M} - and CCS-schemes, respectively, in red and blues lines. The band corresponds to hard function uncertainty.

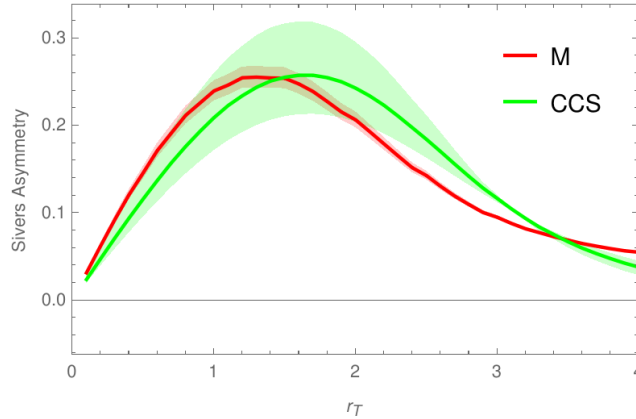


Figure 5: Siivers asymmetry in CCS-scheme (green) and \mathcal{M} -scheme (red).

sensitivity to Collins-Soper kernel differences than the CCS scheme, however, given the current level of precision, the predictions of the two schemes remain compatible within uncertainties.

The results presented so far rely on the ansatz that the gluon Siivers distribution is equal to the sea-quark contribution extracted from fits of the quark Siivers functions. Varying the normalization of this model, including a possible sign change, leads to significantly different predictions, as illustrated

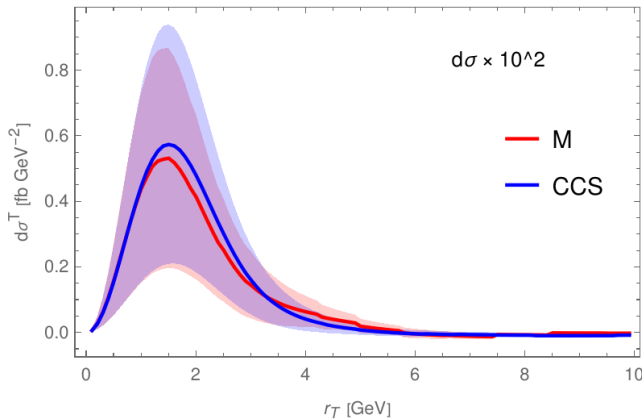


Figure 6: Siverts weighted cross-section with error of the Siverts model in \mathcal{M} - and CCS-scheme, respectively in red and blue lines.

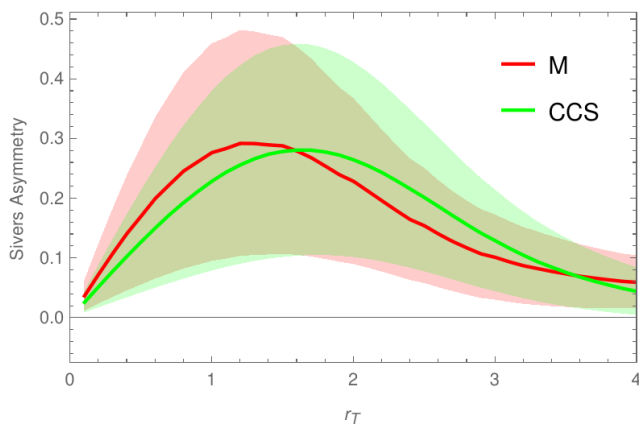


Figure 7: Siverts asymmetry with errors in the Siverts model. In CCS-scheme (green) and \mathcal{M} -scheme (red).

in fig. 8. In particular, setting the gluon Siverts contribution to zero (dashed line in fig. 8) still yields an asymmetry at the level of a few percent. A similar magnitude is obtained when the sign of the gluon Siverts distribution is reversed relative to the default assumption (blue line in fig. 8). An observed asymmetry below the percent level would therefore suggest a nontrivial cancellation between quark and gluon contributions.

10 Conclusions

Dijet cross section in SIDIS is sensitive to gluon distributions. Here we have re-analyzed the unpolarized case and provided the polarized one using TMD factorization at LP, and TMD evolution at $\mathbb{N}^3\text{LO}$. We have identified several sources of uncertainty: scale dependence in hard and collinear-soft functions, nonperturbative inputs of the TMD evolution kernels, scheme dependence of evolution kernels, model dependence of the Siverts functions. All of these items provide hints on the issues that future research must undertake to get a reliable estimations. This includes better perturbative control of hard factors and other functions appearing in the factorization theorem. The results that

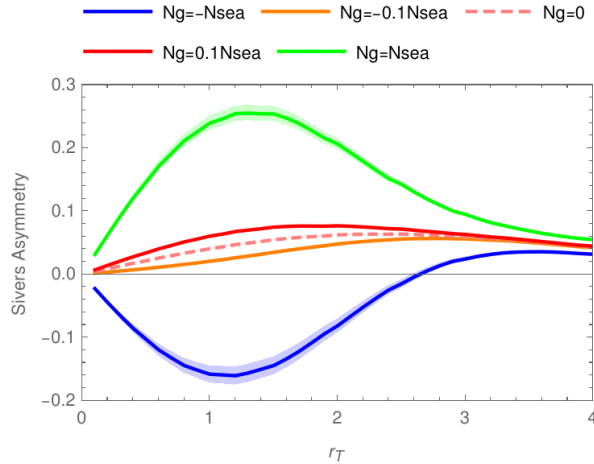


Figure 8: Siverts asymmetry with hard scale variation using the \mathcal{M} -scheme. The gluon-Siverts function has been scaled by different factors in each line. All lines have hard scale variation error bands.

we obtain are still largely model dependent, especially on gluon distributions. As a guideline we have used sea-partonic distributions extracted from previous fits. We are also proposing a resummation scheme (\mathcal{M} -scheme) which is simpler than the one adopted previously in the literature (CCS-scheme) and consistent with ζ -prescription. The scheme is consistent with a SCET-II factorization, but does not resum sum parts which appear in SCET₊ scheme, basically the separation of collinear-soft and jet functions. The latter resummation introduces imaginary parts in the anomalous dimensions that require a sophisticated treatment and limitation on scale factorization intervals [12]. The \mathcal{M} -scheme provides in general smaller errors bands which suggest a better convergence and it is more sensitive to the precise value of the TMD evolution kernel. This suggests that log resummation in collinear-soft and jet function factorization is not as relevant as figured out in theoretical works. More studies are necessary to arrive to more precise statements.

Despite all this, the main indication that we have is that Siverts asymmetry is expected to be large, between 5 to 50% which is clearly interesting phenomenologically and relevant for EIC.

Acknowledgments

We thank Rafael Fernández del Castillo for collaborating in the first stages of this work. P.A.G.G. is supported by the Ministry of Education contract FPI-PRE2020-094385. This project is supported by the Spanish Ministerio de Ciencia, Innovación y Universidades through grants No. PID2022-136510NB-C31 and PID2022-136510NB-C33 funded by MCIN/AEI/10.13039/501100011033, as well as CNS2022-135186. This project is supported as well by the European Union Horizon research MSCA–Staff Exchanges, HORIZON-MSCA-2023-SE-01-101182937-HeI and COST action n. 24159 (SHARP), and by the Basque Government through the grant IT1628-22.

A Appendix

A.1 \mathcal{M} -function saddle point

We have the following equation for $\zeta_\mu^{\mathcal{M}}(b)$:

$$\gamma_{\mathcal{M}\gamma_i}(\mu, \zeta_\mu^{\mathcal{M}}(b)) = 2\mathcal{D}_{\mathcal{M}\gamma_i}(\mu, b) \frac{d\ln\zeta_\mu^{\mathcal{M}}(b)}{d\ln\mu^2}, \quad (\text{A.1})$$

To obtain the perturbative solution of $\zeta_\mu^{\mathcal{M}_{g,q}\text{pert}}(b)$ at first order in α_s we replace the value of $\mathcal{D}_{\mathcal{M}\gamma_i}$ which is the same CS kernel as the TMD. We also replace the value of the anomalous dimension of the total function \mathcal{M} for each channel given by eq. (6.8) and obtain:

$$\begin{aligned} \zeta_\mu^{\mathcal{M}_g\text{pert}} &= \zeta_{2,0}^{\mathcal{M}_g} = \left(\frac{p_T^2 R^2}{\hat{s}}\right)^{2\frac{C_F}{C_A}}, \\ \zeta_\mu^{\mathcal{M}_q\text{pert}} &= \zeta_{2,0}^{\mathcal{M}_q} = \left(\frac{p_T^2 R^2}{\hat{s}}\right)^{\frac{C_F+C_A}{C_F}} \left(\frac{\hat{t}}{\hat{u}}\right)^{\frac{C_F-C_A}{C_F}}, \end{aligned} \quad (\text{A.2})$$

and there is no dependence on the scale μ . To obtain the exact solution we follow the same procedure as in [77], using the change to variable $g = \ln\frac{\zeta}{\zeta_0}$, at the current order (A.1) for the gluon case yields:

$$-4C_A g_0 = 2\mathcal{D}_{\mathcal{M}\gamma_i} \left[-\beta_0 g_0 - \frac{\Gamma_0}{2} g_0' \right]. \quad (\text{A.3})$$

We have so the solution $g_0 = 0$ which brings to

$$\zeta_\mu^{\mathcal{M}_g,\text{exact}} = \zeta_\mu^{\mathcal{M}_g,\text{pert}}, \quad \zeta_\mu^{\mathcal{M}_q,\text{exact}} = \zeta_\mu^{\mathcal{M}_q,\text{pert}}. \quad (\text{A.4})$$

The non null nontrivial solution however does not meet the border conditions that $g = 0$ when $\zeta = \zeta_0$.

A.2 Angular integrals

We express the angular integrals of eq.(6.37-6.38) as

- *Single logarithmic terms,*

$$I_{\log} = \int_{-\pi}^{\pi} d\phi_b \sin^2(\phi_S - \phi_b) \ln(-i\cos\phi_b) = -\frac{\pi}{2} (\cos(2\phi_S) + \ln(4)), \quad (\text{A.5})$$

where,

$$\ln(-i\cos\phi_b) = \ln|\cos\phi_b| - \frac{i\pi}{2} \Theta(\phi_b). \quad (\text{A.6})$$

- *Double logarithmic terms:*

$$I_{\log^2} = \int_{-\pi}^{\pi} d\phi_b \sin^2(\phi_S - \phi_b) \ln^2(-i\cos\phi_b) = -\frac{\pi^3}{6} + \pi \ln^2 2 + \frac{1}{2} \pi \cos(2\phi_S) (1 + \ln 4). \quad (\text{A.7})$$

- *Single Logarithmic A_b terms,*

$$\begin{aligned} I_{A_b} &= \int_{-\pi}^{\pi} d\phi_b \sin^2(\phi_S - \phi_b) \ln(-A_b) \\ &= -\cos 2\phi_s \left[\ln\left(\frac{\hat{s}}{4p_T^2}\right) I_0(1) - 2I_1(1) \right] + \cos^2 \phi_s \left[\ln\left(\frac{\hat{s}}{4p_T^2}\right) I_0(0) - 2I_1(0) \right]. \end{aligned} \quad (\text{A.8})$$

- *Double Logarithmic A_b terms,*

$$I_{A_b^2} = \int_{-\pi}^{\pi} d\phi_b \sin^2(\phi_S - \phi_b) \ln^2(-A_b) = \pi \ln^2 \left(\frac{\hat{s}}{4p_T^2} \right) + 4 \ln \left(\frac{\hat{s}}{4p_T^2} \right) \left(\cos(2\phi_S) I_1(1) - \cos^2 \phi_S I_1(0) \right) + 4 [I_2(0) \cos^2 \phi_S - I_2(1) \cos 2\phi_S], \quad (\text{A.9})$$

with

$$A_b = \frac{(v_1 \cdot v_2)}{2(v_1 \cdot \hat{b})(v_2 \cdot \hat{b})} = -\frac{\hat{s}}{4p_T^2 (\cos \phi_b)^2}. \quad (\text{A.10})$$

- *Poly-logarithmic terms,*

$$\begin{aligned} I_{Li2} &= \int_{-\pi}^{\pi} d\phi_b \sin^2(\phi_S - \phi_b) \text{Li}_2 \left(1 - \frac{\hat{s}}{4p_T^2 \cos^2 \phi_b} \right) \\ &= \int_{-\pi}^{\pi} d\phi_b (-\cos 2\phi_S \cos^2 \phi_b + \cos^2 \phi_S) \text{Li}_2 \left(1 - \frac{1}{\bar{c} \cos^2 \phi_b} \right) \\ &= -\cos 2\phi_S I_{Li}(1, \bar{c}) + \cos^2 \phi_S I_{Li}(0, \bar{c}). \end{aligned} \quad (\text{A.11})$$

We have also used,

$$\Theta(\phi_b) = \begin{cases} +1 & : -\pi/2 < \phi_b < \pi/2, \\ -1 & : \text{otherwise.} \end{cases} \quad (\text{A.12})$$

We also use the following basic integrals:

$$I_n(\mathcal{A}) \equiv \int_{-\pi}^{+\pi} d\phi_b |\cos \phi_b|^{2\mathcal{A}} \ln^n |\cos \phi_b|, \quad (\text{A.13})$$

where

$$\begin{aligned} I_0(\mathcal{A}) &= \frac{2\sqrt{\pi} \Gamma(1/2 + \mathcal{A})}{\Gamma(1 + \mathcal{A})}, \\ I_1(\mathcal{A}) &= \frac{\sqrt{\pi} \Gamma(1/2 + \mathcal{A})}{\Gamma(1 + \mathcal{A})} (H_{\mathcal{A}-1/2} - H_{\mathcal{A}}) \\ I_2(\mathcal{A}) &= \frac{\sqrt{\pi} \Gamma(1/2 + \mathcal{A})}{2\Gamma(1 + \mathcal{A})} \left[(H_{\mathcal{A}-1/2} - H_{\mathcal{A}})^2 + \psi^{(1)} \left(\frac{1}{2} + \mathcal{A} \right) - \psi^{(1)}(1 + \mathcal{A}) \right], \end{aligned} \quad (\text{A.14})$$

where $\mathcal{A} > -1/2$, ψ is the polygamma function and \mathcal{H} is the harmonic function.

B Hard prefactors

The hard prefactors for each channel are given in ref. [31, 54–56],

$$\sigma_0^{gU} = 2\pi p_T \frac{\mathcal{N}}{xs} \frac{A_0^{gU}}{f_1^g(\xi, \mathbf{r}_T)}, \quad \sigma_0^{fU} = 2\pi p_T \frac{\mathcal{N}}{xs} \frac{A_0^{fU}}{f_1^f(\xi, \mathbf{r}_T)}, \quad \sigma_0^{gL} = -4\pi p_T \frac{\mathcal{N}}{xs} \frac{B_2}{h_1^\perp(\xi, \mathbf{r}_T)}, \quad (\text{B.1})$$

where

$$\mathcal{N} = \frac{\alpha^2 \alpha_s}{\pi s p_T^2} \frac{1}{xy^2}, \quad (\text{B.2})$$

$$A_0^{gU} = e_q^2 T_R \left[\left(1 + (1 - y^2) \right) A_{U+L}^{gU} - y^2 A_L^{gU} \right] f_1^g(\xi, \mathbf{r}_T), \quad (\text{B.3})$$

$$A_0^{fU} = e_q^2 C_F \left[\left(1 + (1 - y^2) \right) A_{U+L}^{fU} - y^2 A_L^{fU} \right] f_1^q(\xi, \mathbf{r}_T), \quad (\text{B.4})$$

$$B_2 = e_q^2 T_R \left[\left(1 + (1 - y^2) \right) B_{U+L} - y^2 B_L \right] \frac{r_T^2}{M_p^2} h_1^{\perp g}(\xi, \mathbf{r}_T), \quad (\text{B.5})$$

and A and B factors are given by

$$A_{U+L}^{fU} = \frac{1-z}{D^2} \left\{ 1 + z^2 + [2z(1-z) + 4z^2(1-z)^2] \frac{Q^2}{p_T^2} + [z^2(1-z)^2] [1 + (1-z)^2] \frac{Q^4}{p_T^4} \right\}, \quad (\text{B.6})$$

$$A_{U+L}^{gU} = \frac{1}{D^3} - \frac{z(1-z)}{D^3} \left\{ 2 - 8z(1-z) \frac{Q^2}{p_T^2} - z(1-z)[1 - 2z(1-z)] \frac{Q^4}{p_T^4} \right\}, \quad (\text{B.7})$$

$$B_{U+L} = \frac{z(1-z)}{D^3} \left\{ [1 - 6z(1-z)] \frac{Q^2}{p_T^2} \right\}, \quad (\text{B.8})$$

$$A_L^{fU} = 4 \frac{z^2(1-z)^3}{D^2} \frac{Q^2}{p_T^2}, \quad (\text{B.9})$$

$$A_L^{gU} = 8 \frac{z^2(1-z)^2}{D^3} \frac{Q^2}{p_T^2}, \quad (\text{B.10})$$

$$B_L = -4 \frac{z^2(1-z)^2}{D^3} \frac{Q^2}{p_T^2}, \quad (\text{B.11})$$

where D is defined as

$$D = 1 + z(1-z) \frac{Q^2}{p_T^2}. \quad (\text{B.12})$$

In order to pass from the expressions of cross section of these works to ours we integrate in inelasticity using

$$\int dy \delta(yxs - Q^2).$$

C Anomalous dimensions

The one loop anomalous dimensions used in this paper are

$$\begin{aligned}
\gamma_{H\gamma_g}^{[1]} &= 4 \left\{ C_F \left[\ln \left(\frac{\hat{s}^2}{\mu^4} \right) - 2\gamma_q \right] + C_A \ln \left(\frac{\hat{t} \hat{u}}{\hat{s} \mu^2} \right) \right\}, \\
\gamma_{H\gamma_f}^{[1]} &= 4 \left\{ C_F \left[\ln \left(\frac{\hat{u}^2}{\mu^4} \right) - 2\gamma_q \right] + C_A \ln \left(\frac{\hat{s} \hat{t}}{\hat{u} \mu^2} \right) \right\}, \\
\gamma_{S\gamma_g}^{[1]} &= 4 \left\{ -C_A \ln \zeta_2 + 2C_F \left[\ln(B\mu^2 e^{2\gamma_E}) + \ln \frac{p_T^2}{\hat{s}} + \ln(4c_{\mathbf{b}}^2) \right] \right\}, \\
\gamma_{S\gamma_f}^{[1]} &= 4 \left\{ (C_F + C_A) \left[\ln(B\mu^2 e^{2\gamma_E}) + \ln \frac{p_T^2}{\hat{s}} + \ln(4c_{\mathbf{b}}^2) \right] + (C_F - C_A) \left[\ln \left(\frac{\hat{t}}{\hat{u}} \right) - \kappa(v_f) \right] - C_F \ln \zeta_2 \right\}, \\
\gamma_{F_i}^{[1]} &= 4C_i \left[-\ln \left(\frac{\zeta_1}{\mu^2} \right) + \gamma_i \right], \\
\gamma_{J_i}^{[1]} &= 4C_i \left[-\ln \left(\frac{p_T^2}{\mu^2} \right) - \ln R^2 + \gamma_i \right], \\
\gamma_{C_g}^{[1]} &= 4C_A \left[-\ln \left(B\mu^2 e^{2\gamma_E} \right) + \ln R^2 - \ln(4c_{\mathbf{b}}^2) + \kappa(v_g) \right], \\
\gamma_{C_i}^{[1]} &= 4C_F \left[-\ln \left(B\mu^2 e^{2\gamma_E} \right) + \ln R^2 - \ln(4c_{\mathbf{b}}^2) + \kappa(v_i) \right], \\
\gamma_{\alpha}^{[1]} &= -4C_A \gamma_g, \tag{C.1}
\end{aligned}$$

The imaginary component in the soft and collinear-soft anomalous dimension is denoted by $\kappa(v_i)$ where

$$\kappa(v_f) = -\kappa(v_{\bar{f}}) = -\kappa(v_g) = i\pi \text{sign}(c_{\mathbf{b}}). \tag{C.2}$$

These anomalous dimensions can be found in [11, 12, 60, 62, 83–86].

D Sivers fit parameters

In our results the default values are taken from the DY+SIDIS fit in [64] at N³LO and reported in tab 4.

E Model EKT

The model of ref. [80] is obtained performing first an operator product expansion of the Sivers function onto the Qiu-Sterman function it includes a nonperturbative b_T -dependent correction,

$$f_{iT,\text{EKT}}^\perp(\xi, b; \mu, \zeta) = \left[\bar{C}_{q \leftarrow i} \otimes T_{Fi/p} \right](\xi, b; \mu, \zeta) e^{-g_1^T b^2}, \tag{E.1}$$

where \bar{C} is a Wilson coefficient, perturbatively calculable, and T the nonperturbative Qiu-Sterman function.

Parameter	SIDIS	DY+SIDIS	SIDIS	DY+SIDIS
	at NNLO	at NNLO	at N ³ LO	at N ³ LO
r_0	$0.95^{+0.70}_{-0.94}$	$0.58^{+0.71}_{-0.57}$	$0.94^{+0.71}_{-0.93}$	$0.54^{+0.60}_{-0.53}$
r_1	$0.09^{+5.90}_{-0.09}$	$4.8^{+1.9}_{-3.1}$	$1.02^{+4.96}_{-1.02}$	$5.22^{+1.18}_{-3.43}$
r_2	$195.^{+434.}_{-20.}$	$192.^{+101.}_{-119.}$	$223.^{+409.}_{-47.}$	$203.^{+71.}_{-133.}$
N_u	$-0.013^{+0.008}_{-0.007}$	$-0.020^{+0.013}_{-0.020}$	$-0.012^{+0.007}_{-0.008}$	$-0.017^{+0.011}_{-0.023}$
β_u	$-0.35^{+0.07}_{-0.06}$	$-0.35^{+0.09}_{-0.10}$	$-0.33^{+0.06}_{-0.07}$	$-0.36^{+0.09}_{-0.11}$
ϵ_u	$-3.9^{+0.5}_{-0.3}$	$-3.9^{+0.6}_{-0.6}$	$-3.8^{+0.4}_{-0.4}$	$-3.9^{+0.6}_{-0.6}$
N_d	$0.34^{+0.25}_{-0.21}$	$0.40^{+0.20}_{-0.18}$	$0.34^{+0.25}_{-0.21}$	$0.37^{+0.18}_{-0.17}$
β_d	$-0.77^{+0.61}_{-0.13}$	$-0.51^{+0.70}_{-0.29}$	$-0.82^{+0.66}_{-0.08}$	$-0.7^{+0.77}_{-0.11}$
ϵ_d	$1.8^{+20.0}_{-2.8}$	$9.4^{+13.9}_{-9.9}$	$3.6^{+18.4}_{-4.7}$	$9.0^{+17.6}_{-9.1}$
N_s	$0.43^{+0.42}_{-0.34}$	$0.90^{+0.83}_{-0.56}$	$0.48^{+0.37}_{-0.38}$	$0.76^{+0.89}_{-0.43}$
N_{sea}	$-0.23^{+0.15}_{-0.21}$	$-0.51^{+0.22}_{-0.31}$	$-0.23^{+0.15}_{-0.22}$	$-0.47^{+0.21}_{-0.32}$
$\beta_s = \beta_{\text{sea}}$	$2.3^{+0.7}_{-1.2}$	$2.5^{+0.8}_{-0.7}$	$2.3^{+0.7}_{-1.2}$	$2.5^{+0.8}_{-0.7}$

Table 4: Values of parameters obtained in various fits of ref. [64].

N_u	$0.077^{+0.004}_{-0.005}$ GeV	α_u	$0.967^{+0.028}_{-0.045}$
N_d	$-0.152^{+0.017}_{-0.016}$ GeV	α_d	$1.188^{+0.056}_{-0.023}$
N_s	$0.167^{+0.053}_{-0.051}$ GeV	α_{sea}	$0.936^{+0.069}_{-0.026}$
$N_{\bar{u}}$	$-0.033^{+0.016}_{-0.017}$ GeV	β	$5.129^{+0.017}_{-0.034}$
$N_{\bar{d}}$	$-0.069^{+0.019}_{-0.026}$ GeV	g_1^T	$0.180^{+0.035}_{-0.070}$ GeV ²
$N_{\bar{s}}$	$-0.002^{+0.047}_{-0.040}$ GeV		

Table 5: Fit parameters for ref. [80].

The convolution involves two kinematic variables \hat{x}_1 and \hat{x}_2 and it is given by

$$\left[\bar{C}_{q \leftarrow i} \otimes T_{F i/p} \right] (x, b; \mu, \zeta) = \int_x^1 \frac{d\hat{x}_1}{\hat{x}_1} \frac{d\hat{x}_2}{\hat{x}_2} \bar{C}_{q \leftarrow i}(x/\hat{x}_1, x/\hat{x}_2, b; \mu, \zeta) T_{F i/p}(\hat{x}_1, \hat{x}_2; \mu). \quad (\text{E.2})$$

For $\mu^2 = \mu_{b_*}^2$ the coefficient \bar{C} is

$$\begin{aligned} \bar{C}_{q \leftarrow q'}(x_1, x_2, b; \mu_{b_*}, \mu_{b_*}^2) = & \delta_{qq'} \delta(1-x_1) \delta(1-x_2) - \frac{\alpha_s}{2\pi} \frac{\delta_{qq'}}{2N_C} \delta(1-x_2/x_1) (1-x_1) \\ & - \frac{\alpha_s}{2\pi} \delta_{qq'} C_F \frac{\pi^2}{12} \delta(1-x_1) \delta(1-x_2). \end{aligned} \quad (\text{E.3})$$

and the result of the convolution is:

$$\begin{aligned} \left[\bar{C}_{q \leftarrow i} \otimes T_{F i/p} \right] (x, b; \mu, \zeta) &= \delta_{qi} \left(1 - C_F \frac{\alpha_s \pi^2}{2\pi \cdot 12} \right) T_{F i/p}(x, x; \mu) \\ &\quad - \frac{\alpha_s}{2\pi} \frac{\delta_{qi}}{2N_C} \int_x^1 \frac{d\hat{x}_1}{\hat{x}_1} \left(1 - \frac{x}{\hat{x}_1} \right) T_{F i/p}(\hat{x}_1, \hat{x}_1; \mu). \end{aligned} \quad (\text{E.4})$$

Furthermore, $T_{F q/p}(x, x, \mu)$ is assumed to be proportional to the unpolarized PDF $f_{q/p}(x, \mu_0)$,

$$T_{F q/p}(x, x, \mu) = \mathcal{N}_q(x) f_{q/p}(x, \mu), \quad (\text{E.5})$$

with $\mathcal{N}_q(x)$ given by

$$\mathcal{N}_q(x) = N_q \frac{(\alpha_q + \beta_q)^{(\alpha_q + \beta_q)}}{\alpha_q^{\alpha_q} \beta_q^{\beta_q}} x^{\alpha_q} (1-x)^{\beta_q}. \quad (\text{E.6})$$

The value of the parameters are reported in tab. 5.

References

- [1] R. Angeles-Martinez et al., *Transverse Momentum Dependent (TMD) parton distribution functions: status and prospects*, *Acta Phys. Polon.* **B46** (2015) 2501–2534, [[1507.05267](#)].
- [2] T. Becher and M. Neubert, *Drell-Yan Production at Small q_T , Transverse Parton Distributions and the Collinear Anomaly*, *Eur. Phys. J.* **C71** (2011) 1665, [[1007.4005](#)].
- [3] J. Collins, *Foundations of perturbative QCD*. Cambridge University Press, 2013.
- [4] M. G. Echevarria, A. Idilbi and I. Scimemi, *Soft and Collinear Factorization and Transverse Momentum Dependent Parton Distribution Functions*, *Phys. Lett.* **B726** (2013) 795–801, [[1211.1947](#)].
- [5] J.-Y. Chiu, A. Jain, D. Neill and I. Z. Rothstein, *A Formalism for the Systematic Treatment of Rapidity Logarithms in Quantum Field Theory*, *JHEP* **05** (2012) 084, [[1202.0814](#)].
- [6] A. Vladimirov, V. Moos and I. Scimemi, *Transverse momentum dependent operator expansion at next-to-leading power*, *JHEP* **01** (2022) 110, [[2109.09771](#)].
- [7] P. Caucal, F. Salazar and R. Venugopalan, *Dijet impact factor in DIS at next-to-leading order in the Color Glass Condensate*, *JHEP* **11** (2021) 222, [[2108.06347](#)].
- [8] P. Caucal, F. Salazar, B. Schenke and R. Venugopalan, *Back-to-back inclusive dijets in DIS at small x : Sudakov suppression and gluon saturation at NLO*, *JHEP* **11** (2022) 169, [[2208.13872](#)].
- [9] P. Caucal, F. Salazar, B. Schenke, T. Stebel and R. Venugopalan, *Back-to-Back Inclusive Dijets in Deep Inelastic Scattering at Small x : Complete NLO Results and Predictions*, *Phys. Rev. Lett.* **132** (2024) 081902, [[2308.00022](#)].
- [10] P. Caucal, F. Salazar, B. Schenke, T. Stebel and R. Venugopalan, *Back-to-back inclusive dijets in DIS at small x : gluon Weizsäcker-Williams distribution at NLO*, *JHEP* **08** (2023) 062, [[2304.03304](#)].
- [11] R. F. del Castillo, M. G. Echevarria, Y. Makris and I. Scimemi, *TMD factorization for dijet and heavy-meson pair in DIS*, *JHEP* **01** (2021) 088, [[2008.07531](#)].
- [12] R. F. del Castillo, M. G. Echevarria, Y. Makris and I. Scimemi, *Transverse momentum dependent distributions in dijet and heavy hadron pair production at EIC*, *JHEP* **03** (2022) 047, [[2111.03703](#)].
- [13] C. W. Bauer, S. Fleming, D. Pirjol and I. W. Stewart, *An Effective field theory for collinear and soft gluons: Heavy to light decays*, *Phys. Rev. D* **63** (2001) 114020, [[hep-ph/0011336](#)].

- [14] C. W. Bauer, D. Pirjol and I. W. Stewart, *Soft collinear factorization in effective field theory*, *Phys. Rev. D* **65** (2002) 054022, [[hep-ph/0109045](#)].
- [15] C. W. Bauer, S. Fleming, D. Pirjol, I. Z. Rothstein and I. W. Stewart, *Hard scattering factorization from effective field theory*, *Phys. Rev. D* **66** (2002) 014017, [[hep-ph/0202088](#)].
- [16] M. Beneke, A. P. Chapovsky, M. Diehl and T. Feldmann, *Soft collinear effective theory and heavy to light currents beyond leading power*, *Nucl. Phys. B* **643** (2002) 431–476, [[hep-ph/0206152](#)].
- [17] T. Becher, A. Broggio and A. Ferroglia, *Introduction to Soft-Collinear Effective Theory*, *Lect. Notes Phys.* **896** (2015) pp.1–206, [[1410.1892](#)].
- [18] R. Abdul Khalek et al., *Science Requirements and Detector Concepts for the Electron-Ion Collider: EIC Yellow Report*, **2103.05419**.
- [19] S. Rodini and A. Vladimirov, *Transverse momentum dependent factorization for SIDIS at next-to-leading power*, *Phys. Rev. D* **110** (2024) 034009, [[2306.09495](#)].
- [20] R. F. del Castillo, M. Jaarsma, I. Scimemi and W. Waalewijn, *Transverse momentum measurements with jets at next-to-leading power*, *JHEP* **02** (2024) 074, [[2307.13025](#)].
- [21] M. Jaarsma, O. del Rio, I. Scimemi and W. Waalewijn, *Soft background fields at next-to-leading power in transverse momentum dependent SIDIS with jets*, *JHEP* **11** (2025) 014, [[2507.03072](#)].
- [22] S. Piloneta and A. Vladimirov, *Kinematic power corrections for TMD factorization theorem of semi-inclusive deep-inelastic scattering*, **2510.14496**.
- [23] D. Boer, C. Lorcé, C. Pisano and J. Zhou, *The gluon Sivers distribution: status and future prospects*, *Adv. High Energy Phys.* **2015** (2015) 371396, [[1504.04332](#)].
- [24] P. Mulders and J. Rodrigues, *Transverse momentum dependence in gluon distribution and fragmentation functions*, *Phys. Rev. D* **63** (2001) 094021, [[hep-ph/0009343](#)].
- [25] U. D’Alesio, F. Murgia, C. Pisano and P. Taels, *Probing the gluon Sivers function in $p^\uparrow p \rightarrow J/\psi X$ and $p^\uparrow p \rightarrow DX$* , *Phys. Rev. D* **96** (2017) 036011, [[1705.04169](#)].
- [26] U. D’Alesio, C. Flore, F. Murgia, C. Pisano and P. Taels, *Unraveling the Gluon Sivers Function in Hadronic Collisions at RHIC*, *Phys. Rev. D* **99** (2019) 036013, [[1811.02970](#)].
- [27] U. D’Alesio, L. Maxia, F. Murgia, C. Pisano and S. Rajesh, *Process dependence of the gluon Sivers function in $p^\uparrow p \rightarrow J/\psi + X$ within a TMD scheme in NRQCD*, *Phys. Rev. D* **102** (2020) 094011, [[2007.03353](#)].
- [28] LHCSPIN collaboration, A. Accardi et al., *LHCspin: a Polarized Gas Target for LHC*, **2504.16034**.
- [29] F. Yuan, *Heavy Quarkonium Production in Single Transverse Polarized High Energy Scattering*, *Phys. Rev. D* **78** (2008) 014024, [[0801.4357](#)].
- [30] R. M. Godbole, A. Kaushik, A. Misra and V. S. Rawoot, *Transverse single spin asymmetry in $e + p^\uparrow \rightarrow e + J/\psi + X$ and Q^2 evolution of Sivers function-II*, *Phys. Rev. D* **91** (2015) 014005, [[1405.3560](#)].
- [31] D. Boer, P. J. Mulders, C. Pisano and J. Zhou, *Asymmetries in Heavy Quark Pair and Dijet Production at an EIC*, *JHEP* **08** (2016) 001, [[1605.07934](#)].
- [32] A. Mukherjee and S. Rajesh, *J/ψ production in polarized and unpolarized ep collision and Sivers and $\cos 2\phi$ asymmetries*, *Eur. Phys. J. C* **77** (2017) 854, [[1609.05596](#)].
- [33] A. Bacchetta, D. Boer, C. Pisano and P. Taels, *Gluon TMDs and NRQCD matrix elements in J/ψ production at an EIC*, *Eur. Phys. J. C* **80** (2020) 72, [[1809.02056](#)].

- [34] L. Zheng, E. Aschenauer, J. Lee, B.-W. Xiao and Z.-B. Yin, *Accessing the gluon Sivers function at a future electron-ion collider*, *Phys. Rev. D* **98** (2018) 034011, [[1805.05290](#)].
- [35] U. D’Alesio, F. Murgia, C. Pisano and P. Tael, *Azimuthal asymmetries in semi-inclusive J/ψ + jet production at an EIC*, *Phys. Rev. D* **100** (2019) 094016, [[1908.00446](#)].
- [36] A. Bacchetta, F. G. Celiberto and M. Radici, *T-odd gluon distribution functions in a spectator model*, *Eur. Phys. J. C* **84** (2024) 576, [[2402.17556](#)].
- [37] I. Scimemi and A. Vladimirov, *Systematic analysis of double-scale evolution*, *JHEP* **08** (2018) 003, [[1803.11089](#)].
- [38] “artemide web-page, <https://teorica.fis.ucm.es/artemide/> artemide repository, <https://github.com/vladimirovalexy/artemide-public>.”
- [39] I. Scimemi and A. Vladimirov, *Analysis of vector boson production within TMD factorization*, *Eur. Phys. J. C* **78** (2018) 89, [[1706.01473](#)].
- [40] V. Bertone, I. Scimemi and A. Vladimirov, *Extraction of unpolarized quark transverse momentum dependent parton distributions from Drell-Yan/Z-boson production*, *JHEP* **06** (2019) 028, [[1902.08474](#)].
- [41] I. Scimemi and A. Vladimirov, *Non-perturbative structure of semi-inclusive deep-inelastic and Drell-Yan scattering at small transverse momentum*, *JHEP* **06** (2020) 137, [[1912.06532](#)].
- [42] V. Moos, I. Scimemi, A. Vladimirov and P. Zurita, *Extraction of unpolarized transverse momentum distributions from the fit of Drell-Yan data at N^4LL* , *JHEP* **05** (2024) 036, [[2305.07473](#)].
- [43] V. Moos, I. Scimemi, A. Vladimirov and P. Zurita, *Determination of unpolarized TMD distributions from the fit of Drell-Yan and SIDIS data at N^4LL* , [2503.11201](#).
- [44] M. Bury, A. Prokudin and A. Vladimirov, *Extraction of the Sivers function from SIDIS, Drell-Yan, and W^\pm/Z boson production data with TMD evolution*, *JHEP* **05** (2021) 151, [[2103.03270](#)].
- [45] MAP (MULTI-DIMENSIONAL ANALYSES OF PARTONIC DISTRIBUTIONS) collaboration, A. Bacchetta, V. Bertone, C. Bissolotti, G. Bozzi, M. Cerutti, F. Piacenza et al., *Unpolarized transverse momentum distributions from a global fit of Drell-Yan and semi-inclusive deep-inelastic scattering data*, *JHEP* **10** (2022) 127, [[2206.07598](#)].
- [46] MAP (MULTI-DIMENSIONAL ANALYSES OF PARTONIC DISTRIBUTIONS) collaboration, R. A. Khalek, V. Bertone and E. R. Nocera, *Determination of unpolarized pion fragmentation functions using semi-inclusive deep-inelastic-scattering data*, *Phys. Rev. D* **104** (2021) 034007, [[2105.08725](#)].
- [47] MAP (MULTI-DIMENSIONAL ANALYSES OF PARTONIC DISTRIBUTIONS) collaboration, A. Bacchetta, V. Bertone, C. Bissolotti, G. Bozzi, M. Cerutti, F. Delcarro et al., *Flavor dependence of unpolarized quark transverse momentum distributions from a global fit*, *JHEP* **08** (2024) 232, [[2405.13833](#)].
- [48] Z.-B. Kang, K. Lee, D. Y. Shao and J. Terry, *The Sivers Asymmetry in Hadronic Dijet Production*, [2008.05470](#).
- [49] Y.-T. Chien, R. Rahn, D. Y. Shao, W. J. Waalewijn and B. Wu, *Precision boson-jet azimuthal decorrelation at hadron colliders*, *JHEP* **02** (2023) 256, [[2205.05104](#)].
- [50] R.-J. Fu, R. Rahn, D. Y. Shao, W. J. Waalewijn and B. Wu, *Resummed azimuthal decorrelation and transverse momentum imbalance of dijets at the LHC*, [2602.20249](#).
- [51] D. Gutierrez-Reyes, S. Leal-Gomez, I. Scimemi and A. Vladimirov, *Linearly polarized gluons at next-to-next-to leading order and the Higgs transverse momentum distribution*, *JHEP* **11** (2019) 121, [[1907.03780](#)].
- [52] M. G. Echevarria, T. Kasemets, P. J. Mulders and C. Pisano, *QCD evolution of (un)polarized gluon TMDPDFs and the Higgs q_T -distribution*, *JHEP* **07** (2015) 158, [[1502.05354](#)].

- [53] D. Boer, S. Cotogno, T. van Daal, P. J. Mulders, A. Signori and Y.-J. Zhou, *Gluon and Wilson loop TMDs for hadrons of spin ≤ 1* , *JHEP* **10** (2016) 013, [[1607.01654](#)].
- [54] C. Pisano, D. Boer, S. J. Brodsky, M. G. A. Buffing and P. J. Mulders, *Linear polarization of gluons and photons in unpolarized collider experiments*, *JHEP* **10** (2013) 024, [[1307.3417](#)].
- [55] A. V. Efremov, N. Y. Ivanov and O. V. Teryaev, *How to measure the linear polarization of gluons in unpolarized proton using the heavy-quark pair lepton production*, *Phys. Lett. B* **777** (2018) 435–441, [[1711.05221](#)].
- [56] A. V. Efremov, N. Y. Ivanov and O. V. Teryaev, *The ratio $R = d\sigma_L/d\sigma_T$ in heavy-quark pair lepton production as a probe of linearly polarized gluons in unpolarized proton*, *Phys. Lett. B* **780** (2018) 303–307, [[1801.03398](#)].
- [57] I. Scimemi and A. Vladimirov, *Matching of transverse momentum dependent distributions at twist-3*, *Eur. Phys. J. C* **78** (2018) 802, [[1804.08148](#)].
- [58] J.-y. Chiu, A. Fuhrer, A. H. Hoang, R. Kelley and A. V. Manohar, *Soft-Collinear Factorization and Zero-Bin Subtractions*, *Phys. Rev. D* **79** (2009) 053007, [[0901.1332](#)].
- [59] M. G. Echevarria, A. Idilbi and I. Scimemi, *Factorization Theorem For Drell-Yan At Low q_T And Transverse Momentum Distributions On-The-Light-Cone*, *JHEP* **07** (2012) 002, [[1111.4996](#)].
- [60] M. G. Echevarria, I. Scimemi and A. Vladimirov, *Universal transverse momentum dependent soft function at NNLO*, *Phys. Rev. D* **93** (2016) 054004, [[1511.05590](#)].
- [61] M. G. Echevarria, I. Scimemi and A. Vladimirov, *Unpolarized Transverse Momentum Dependent Parton Distribution and Fragmentation Functions at next-to-next-to-leading order*, *JHEP* **09** (2016) 004, [[1604.07869](#)].
- [62] M. G. Buffing, Z.-B. Kang, K. Lee and X. Liu, *A transverse momentum dependent framework for back-to-back photon+jet production*, [[1812.07549](#)].
- [63] A. Hornig, Y. Makris and T. Mehen, *Jet shapes in dijet events at the lhc in scet*, *Journal of High Energy Physics* **2016** (Apr, 2016) 1?41.
- [64] M. Bury, A. Prokudin and A. Vladimirov, *Extraction of the Sivers Function from SIDIS, Drell-Yan, and W^\pm/Z Data at Next-to-Next-to-Next-to Leading Order*, *Phys. Rev. Lett.* **126** (2021) 112002, [[2012.05135](#)].
- [65] MAP (MULTI-DIMENSIONAL ANALYSES OF PARTONIC DISTRIBUTIONS) collaboration, A. Bacchetta, V. Bertone, C. Bissolotti, M. Cerutti, M. Radici, S. Rodini et al., *Neural-Network Extraction of Unpolarized Transverse-Momentum-Dependent Distributions*, *Phys. Rev. Lett.* **135** (2025) 021904, [[2502.04166](#)].
- [66] D. Bollweg, X. Gao, S. Mukherjee and Y. Zhao, *Nonperturbative Collins-Soper kernel from chiral quarks with physical masses*, *Phys. Lett. B* **852** (2024) 138617, [[2403.00664](#)].
- [67] A. Avkhadiev, P. E. Shanahan, M. L. Wagman and Y. Zhao, *Collins-Soper kernel from lattice QCD at the physical pion mass*, *Phys. Rev. D* **108** (2023) 114505, [[2307.12359](#)].
- [68] A. Avkhadiev, P. E. Shanahan, M. L. Wagman and Y. Zhao, *Determination of the Collins-Soper Kernel from Lattice QCD*, *Phys. Rev. Lett.* **132** (2024) 231901, [[2402.06725](#)].
- [69] H.-T. Shu, M. Schlemmer, T. Sizmann, A. Vladimirov, L. Walter, M. Engelhardt et al., *Universality of the Collins-Soper kernel in lattice calculations*, *Phys. Rev. D* **108** (2023) 074519, [[2302.06502](#)].
- [70] LATTICE PARTON (LPC) collaboration, M.-H. Chu et al., *Nonperturbative determination of the Collins-Soper kernel from quasitransverse-momentum-dependent wave functions*, *Phys. Rev. D* **106** (2022) 034509, [[2204.00200](#)].

- [71] CASCADE collaboration, S. Baranov et al., *CASCADE3 A Monte Carlo event generator based on TMDs*, *Eur. Phys. J. C* **81** (2021) 425, [[2101.10221](#)].
- [72] A. Bermudez Martinez et al., *The transverse momentum spectrum of low mass Drell–Yan production at next-to-leading order in the parton branching method*, *Eur. Phys. J. C* **80** (2020) 598, [[2001.06488](#)].
- [73] A. Bermudez Martinez and A. Vladimirov, *Determination of the Collins-Soper kernel from cross-sections ratios*, *Phys. Rev. D* **106** (2022) L091501, [[2206.01105](#)].
- [74] W.-Y. Liu, I. Zahed and Y. Zhao, *Collins-Soper kernel in the QCD instanton vacuum*, *Phys. Rev. D* **111** (2025) 074022, [[2501.00678](#)].
- [75] M. Boglione and A. Simonelli, *Full treatment of the thrust distribution in single inclusive $e+e$ -to $h X$ processes*, *JHEP* **09** (2023) 006, [[2306.02937](#)].
- [76] F. Aslan, M. Boglione, J. O. Gonzalez-Hernandez, T. Rainaldi, T. C. Rogers and A. Simonelli, *Phenomenology of TMD parton distributions in Drell-Yan and $Z0$ boson production in a hadron structure oriented approach*, *Phys. Rev. D* **110** (2024) 074016, [[2401.14266](#)].
- [77] A. Vladimirov, *Pion-induced Drell-Yan processes within TMD factorization*, *JHEP* **10** (2019) 090, [[1907.10356](#)].
- [78] I. Moutl, H. X. Zhu and Y. J. Zhu, *The four loop QCD rapidity anomalous dimension*, *JHEP* **08** (2022) 280, [[2205.02249](#)].
- [79] C. Duhr, B. Mistlberger and G. Vita, *Four-Loop Rapidity Anomalous Dimension and Event Shapes to Fourth Logarithmic Order*, *Phys. Rev. Lett.* **129** (2022) 162001, [[2205.02242](#)].
- [80] M. G. Echevarria, Z.-B. Kang and J. Terry, *Global analysis of the Sivers functions at NLO+NNLL in QCD*, *JHEP* **01** (2021) 126, [[2009.10710](#)].
- [81] U. D’Alesio, F. Murgia and C. Pisano, *Towards a first estimate of the gluon Sivers function from A_N data in pp collisions at RHIC*, *JHEP* **09** (2015) 119, [[1506.03078](#)].
- [82] A. Bacchetta, F. G. Celiberto, M. Radici and P. Taelts, *Transverse-momentum-dependent gluon distribution functions in a spectator model*, *Eur. Phys. J. C* **80** (2020) 733, [[2005.02288](#)].
- [83] T. Becher and M. D. Schwartz, *Direct photon production with effective field theory*, *JHEP* **02** (2010) 040, [[0911.0681](#)].
- [84] T. Becher, C. Lorentzen and M. D. Schwartz, *Precision Direct Photon and W -Boson Spectra at High p_T and Comparison to LHC Data*, *Phys. Rev. D* **86** (2012) 054026, [[1206.6115](#)].
- [85] Y.-T. Chien, R. Rahn, S. Schrijnder van Velzen, D. Y. Shao, W. J. Waalewijn and B. Wu, *Azimuthal angle for boson-jet production in the back-to-back limit*, [2005.12279](#).
- [86] A. Hornig, Y. Makris and T. Mehen, *Jet Shapes in Dijet Events at the LHC in SCET*, *JHEP* **04** (2016) 097, [[1601.01319](#)].